Title: Pathogenicity effector candidates and accessory genome revealed by pan-genomic analysis of *Parastagonospora nodorum*.

Short Title: *Parastagonospora nodorum* pan-genomics

Darcy A. B. Jones[1#], Kasia Rybak[1], Stefania Bertazzoni[1], Kar-Chun Tan[1], Huyen T. T. Phan[1], and James K. Hane[1,2*#]

[1] Centre for Crop & Disease Management, School of Molecular & Life Sciences, Curtin University, Perth, Australia

[2] Curtin Institute for Computation, Curtin University, Perth, Australia

* Corresponding author: james.hane@curtin.edu.au

Keywords: Fungi, Plant Pathogen, Pathogenicity Effector, Parastagonospora nodorum, Pan-genome

Abstract

The wheat pathogen *Parastagonospora nodorum* has emerged as a model necrotrophic fungal species with growing genomic resources. Recent population-level pan-genome studies were leveraged to provide novel insights into pathogen evolution and effector-like gene contents relevant to local crop disease outbreaks. In this study, we examined 156 isolates representing a regional population from the Western Australian (WA) wheat-belt region, and 17 internationally sourced isolates. We observed a highly diverse local population, within which were numerous small and highly similar clusters of isolates from hotter and drier regions. Pan-genome assembly and orthologous gene datasets resulted in 3579 predicted effector candidates, 2291 of which exhibited presence-absence variation (PAV) across the population, and 1362 were specific to WA isolates. There was an abundance of mutations (including repeat-induced point mutation (RIP)), distributed in 'hot-spots' within the pan-genomic landscape that were rich in effector candidates. Three characterised effector loci (*ToxA*, *Tox1* and *Tox3*) were located within sub-telomeric regions of lower diversity, but were nestled within larger high-diversity regions. RIP was widespread across the genome, but non-synonymous RIP-like mutations were strongly selected against. These improved bioinformatic resources for *P. nodorum*, represent progressive advancements in fungal pan-genomics, with a view towards supporting region-specific surveillance of host-pathogen interactions.

Introduction

Parastagonospora nodorum is a necrotrophic pathogen causing septoria nodorum blotch (SNB) of wheat (*Triticum spp.*) (Solomon et al. 2006) which leads to significant yield losses in Australia (Murray and Brennan 2009). *P. nodorum* is primarily spread by infected seed, infested debris or by wind dispersed sexual ascospores (Solomon et al. 2006). Secondary infections can occur when water splash spreads asexual pycnidiospores to higher leaves and glumes, causing further necrotic patches and crop loss. *P. nodorum* is observed to be highly diverse in the field (Stukenbrock et al. 2006, McDonald et al. 2012), and appears to regularly reproduce sexually (Murphy et al. 2000, Bathgate and Loughman 2001, Sommerhalder et al. 2006). This suggests a high adaptive capacity of *P. nodorum* populations, where application of strong selective pressures may be quickly overcome by extant diversity.

P. nodorum infection heavily relies on the activity of necrotrophic effector proteins (NEs), which are secreted into the host and cause cell death upon recognition by host susceptibility (S)-proteins (Tan et al. 2010). Three NEs have been characterised in *P. nodorum* to date: ToxA (Liu et al. 2006), Tox1 (Liu et al. 2012) and Tox3 (Liu et al. 2009). At least five additional host specific necrosis phenotypic interactions have been described in the *P. nodorum*-wheat pathosystem (Friesen et al. 2007, Friesen et al. 2008, Abeysekara et al. 2009, Zhang et al. 2011, Friesen et al. 2012, Gao et al. 2015, Shi et al. 2015, Phan et al. 2018), indicating the presence of additional undiscovered NEs. Identification of the *ToxA* NE has led to deployment of a ToxA resistant wheat cultivar (Tan et al. 2014), and the presence of additional major disease resistance quantitative trait loci (QTL) encourages further development of disease resistant cultivars. However, the known epistatic interactions of Tox1 and Tox2 over Tox3 (Friesen et al. 2007, Phan et al. 2016) indicates that the contributions of different effector-receptor interactions to virulence are complex, and that reliable markers of S-genes and knowledge of the epistasis interactions are important for future disease breeding efforts. The discovery of novel NEs in *P. nodorum* (and other fungal pathogens) remains an important element of crop protection research (Vleeshouwers and Oliver 2014). Fungal effector discovery relies heavily on genomic and bioinformatic resources (Jones et al. 2018), and the increased accessibility of sequencing has resulted in a considerable increase in the rate of effector discovery (Kanja and Hammond-Kosack 2020).

P. nodorum was among the first fungal species for which a reference genome sequence was generated (for the Western Australian (WA) isolate SN15) (Hane et al. 2007), and was the first species within the class Dothideomycetes, which comprises several prominent cereal necrotroph and hemibiotroph species (Ohm et al. 2012, Aylward et al. 2017). The SN15 reference isolate has predominated molecular plant pathology studies of *P. nodorum* since, becoming an important model for the cereal necrotrophs (Solomon et al. 2006). Significant resources have accumulated over time for the SN15 isolate and *P. nodorum* in general, including transcriptomic (Hane et al. 2007, Ipcho et al. 2012, Syme et al. 2016, Richards et al. 2018, Jones et al. 2019), proteomic (Bringans et al. 2009, Syme et al. 2016), and metabolomic (Lowe et al. 2008, Gummer et al. 2013, Chooi et al. 2014, Muria-Gonzalez et al. 2020) datasets. Notable recent additions to the growing pool of *P. nodorum* data include the chromosome-scale genome assemblies of SN15 and 3 other reference isolates (Richards et al. 2018, Bertazzoni et al. 2021).

Parastagonospora nodorum pan-genomics

Improving cost and availability of genome and transcriptome sequencing has significantly advanced plant pathology, enabling conceptual shifts from the focused study of a single reference isolate, to large-scale comparative genomics between numerous isolates over a few short years. Three pan-genomic comparative studies of *P. nodorum* have been conducted to date, comparing global collections of isolates (Syme et al. 2018, Pereira et al. 2020, Bertazzoni et al. 2021), and populations within the USA (Richards et al. 2019). Syme *et al*. (Syme et al. 2018) compared the genomes of *P. nodorum* isolates from Iran, Finland, Sweden, Switzerland, South Africa, the USA, and Australia. They observed frequent presence-absence variation in the effectors *ToxA*, *Tox1*, and *Tox3*, and possible accessory genomic regions with potential roles in virulence. Additionally, numerous genes were observed to be under positive selection pressure, including several effector candidate proteins. They observed distinct regions with large numbers of mutations and some regions with consistently high dN/dS ratios, indicating positive selection and enrichment of adaptively relevant genes in specific genomic regions. Pereira *et al*. (Pereira et al. 2020) sequenced the genomes of *P. nodorum* isolates from Australia, Iran, South Africa, Switzerland, and the USA to investigate *P. nodorum* adaptation to fungicide use. The highest genetic diversity was found in the Iranian population, consistent with the hypothesis that *P. nodorum* co-evolved with wheat during early domestication (Ghaderi et al. 2020), while low diversity was observed within the Australian isolates. A genome-wide association study identified several loci correlated with azole resistance, with higher incidence of fungicide resistance and the identified resistance associated alleles in the Swiss population. Richards *et al*. (Richards et al. 2019) sequenced 197 *P. nodorum* isolates collected from Spring, Winter and Durum wheat cultivars across the growing region of the USA. Two major US sub-populations were identified corresponding to geographical features and wheat lines grown, with one sub-population almost completely lacking *ToxA*. Both populations had diversified at different loci, indicating distinct selective pressures and resulting in different sets of effector candidates predicted by genome-wide association. The USA population study also highlighted several patterns of gene presence-absence variation (PAV) between isolates. The known effector genes *ToxA, Tox1 and Tox3* were absent in 37%, 5% and 41% of US isolates respectively. Gene PAV was commonly associated with transposons in USA isolates, yet there was no significant association with frequency of secreted or effector-like proteins.

Collectively, these genomic studies have highlighted the high diversity of *P. nodorum* genomes, and that studies focusing only on reference isolates are missing considerable amounts of

information. The 400 kb accessory chromosome 23 (AC23), which is missing in the avirulent isolate Sn79-1087, may have a role in host-specific virulence (Bertazzoni et al. 2018) and has a high background rate of mutation (Richards et al. 2018, Bertazzoni et al. 2021). Similarly, regional biases for high AT-base content and RIP-like activity suggests the presence of rapidly mutating accessory regions, primarily within repeat-rich stretches of AC23 and sub-telomeric regions (Richards et al. 2018, Syme et al. 2018, Bertazzoni et al. 2021). Numerous effector candidates have been derived from these genomic studies, utilising features such as signatures of positive selection across isolates, similarity to known effectors, signal peptides, EffectorP results (Sperschneider et al. 2016, Sperschneider et al. 2018), genomic context (e.g. AT-richness or distance to TEs), presence or absence in avirulent isolates, and genome wide association (Richards et al. 2018, Syme et al. 2018, Richards et al. 2019, Bertazzoni et al. 2021). In the Australian reference isolate SN15, many of these genomic features have been combined with a broad range of experimental and bioinformatic indicators to refine effector candidate lists, including: *in planta* gene expression (Jones et al. 2019), putative lateral gene transfer with other cereal-pathogenic fungi (https://effectordb.com), and predicted effector-like gene and protein properties (Syme et al. 2018, Bertazzoni et al. 2021).

The Western Australian *P. nodorum* pan-genome

Despite the long history of study of the Australian *P. nodorum* reference isolate SN15, relatively little was known about the genomic diversity of the *P. nodorum* population in WA until recently. A study of 28 SSR loci compared a WA population of 155 isolates collected over 44 years, and contrasted this population with 23 international isolates sourced from France and the USA (Phan et al. 2020). This SSR study identified two core admixed clusters in WA, with three low-diversity satellite clusters that were geographically and temporally restricted. The population shift broadly correlated with historical shifts in wheat cultivar preference, particularly after the mass adoption of the ToxA insensitive cultivar “Mace” in 2013 which covers nearly 70% of the area sown (Trainor et al. 2018). Although wheat cultivar disease resistance has increased over time, more recently sampled isolates from emergent clusters were more pathogenic than older isolates.

In this study, we further dissect the evolutionary history of a WA *P. nodorum* population previously analysed by Phan *et al*. (Phan et al. 2020) using whole genome sequencing. Further, we compare these genomes with isolates previously sequenced by Syme *et al*. (Syme et al. 2018), and identify novel effector candidates in *P. nodorum*. Guided by phylogeographic and

146 population structure analyses, we observe a highly diverse population in WA, with numerous
147 small highly similar clusters collected from hotter and drier regions of Western Australia. We
148 present the first report of novel sequences and genes within the growing pool of *P. nodorum*
149 pangenome data, specific to locally-adapted isolates. We also combine new WA pangenome
150 data with existing resources to define new effector candidate orthologous groups, extending
151 effector candidate discovery beyond reference isolates. Overall, this growing wealth of new
152 pathogen population data has enhanced our understanding of the pathogenicity gene content,
153 genome architecture and population dynamics for the model cereal necrotroph, *P. nodorum*.

154

Results

Quality control of input sequence data

A total of 156 Western Australian *P. nodorum* isolates described previously (Syme et al. 2018, Phan et al. 2020) were sequenced using short-read Illumina sequencing. The majority of sequencing read pairs were assigned by Kraken2 to either *Parastagonospora nodorum* (average 74.1%) or were unclassified (average 25.6%) (table S2). A small number of read pairs matched other organisms across kingdoms, but no fastq files had more than 1% of reads assigned to any non-fungal taxon nor were any consistent trends observed. Sequencing read quality was generally high, with only a single lane of sequencing (of three) for the isolate WAC13068 failing QC because of low base quality (data S1). Mean insert sizes for isolates sequenced with 125 bp reads ranged between 441 and 709 bp (mean 632 bp), with standard deviations between 263bp and 760bp. Insert sizes for isolates sequenced with 150bp reads varied between 275bp and 321bp (mean 305 bp) with standard deviations between 208 bp and 295 bp.

Prediction of mutations across the *P. nodorum* pan-genome relative to the SN15 reference isolate

Short variants (SNPs, insertions, and deletions) were predicted from aligned short-read sequenced isolates from this study and 15 previously published additional isolates (Syme et al. 2018) (table S1) using the SN15 genome as a reference (Bertazzoni et al. 2021), yielding 895,000 variant loci after filtering (table S3, data S2-S8) corresponding to 1 mutation for every 41 bases in the genome on average. The majority of variants were SNPs (830,761), compared to 33,943 and 30,296 insertions and deletions. Most SNPs were C↔T or G↔A mutations (296,688 and 296,927, respectively), with an overall transition to transversion ratio of 2.5. Relative to the genome of the SN15 reference isolate, 7.4% of variants were within exon features, 3236 mutations resulted in truncation (gain of stop), 660 mutations resulted in loss of a stop codon, 466 mutations resulting in loss of start codon, 249 and 310 mutations were in splice

site acceptor or donor sites respectively, 9896 were frameshift variants, 148,914 were missense mutations, 205,602 were synonymous variants, and there were 1648 and 1591 disruptive in-frame deletions and insertions, respectively.

Phylogeny and structure of the local Western Australian *P. nodorum* population

A subset of SNPs for phylogenetic and population genetics analyses were selected (maximum missing genotypes of 30%, minimum non-major allele frequency of 0.05, and filtering correlated loci within 10 Kb) resulting in 45,194 SNP loci from all illumina sequenced isolates.
A phylogenetic tree was estimated from these SNPs using IQTree (Minh et al. 2020) (Fig 1). The resulting tree grouped isolates from WA and non-Australian isolates into distinct clades. Leaf lengths were generally long within the WA clade, however, six groups of isolates with very short branch lengths were observed, with sizes ranging from 3 to 14 isolates (Data S9, Fig S1). Some internal tree nodes had low UFBoot support values (< 95), indicating that some of the high level relationships were poorly resolved. A major split with high SH-aLRT but low UFBoot support was observed, which tended to separate isolates with long branch lengths from a diverse range of locations from a second clade comprised mostly of several highly similar clades which were generally collected from northern regions of the WA wheat growing area (Geraldton and Dandaragan). No obvious correspondence between effector haplotype profiles and high level phylogenetic clades was observed; but at lower level clades effector haplotype profiles appear to be conserved, particularly where member isolates have short branch lengths (Fig 1).

Analysis of population structure from SNP data with STRUCTURE (Fig 1, Table S4), predicted nine clusters, with the non-Australian isolates forming a single cluster (Structure cluster 8). Within the WA isolates, a single main population was observed (cluster 4) with 7 small satellite clusters. Few isolates were unambiguously assigned to the main cluster (21 of 102 had a posterior probability of > 0.85), with small but appreciable posterior probabilities contributed by satellite clusters and the international cluster. Noting this, we refer to isolates with the highest posterior probability of assignment to cluster 4 as members. These members generally had long branch lengths in the phylogenetic tree and were found in multiple clades. This main cluster corresponds to the two main clusters (1 and 2) presented in Phan et al. (Phan et al. 2020) (referred to hereafter as clusters P1-5) (Fig S2 and S3). The seven remaining clusters identified

by STRUCTURE corresponded to clades in the phylogenetic tree where all leaves had very short lengths, indicating that all members were highly similar to each other. Cluster 1 consists of 3 isolates collected from Geraldton in 2012 (Fig S4 and S5). Cluster 2 consists of 8 isolates collected from Geraldton in 2005 and 2011. Cluster 3 consists of 14 isolates collected from Geraldton in 2005, 2011, and 2012. Cluster 5 consists of 5 isolates collected from Geraldton in 2005 and 2011. Cluster 6 consists of 7 isolates collected from Geraldton, South Perth, or WA (unknown specific location) between the years 1980 and 2011. Cluster 9 consists of 12 isolates collected from Mingenew (near Geraldton) or WA in 2016. Clusters 3, 6, and 9 correspond to the satellite clusters P3, P4, and P5 presented by Phan *et al.* (Phan et al. 2020), respectively. The remaining clusters further separate the main populations identified by Phan *et al*. (Phan et al. 2020), with cluster 1 separating from P2, and clusters 7, 5, and 2 separating from P1. The Tox1 effector haplotypes of members in cluster 5 were highly variable and contained rare variants in the WA population.

Population diversity statistics indicated that individuals within clusters except the core WA cluster (4) and the international cluster (8) are highly similar (Table 1, Table S4). F_{ST} and average locus expected heterozygosity suggests that the alleles are nearly fixed in these clusters. The mean locus G'_{ST} (a normalised variant of F_{ST} that accounts for multi-allelic markers) (Hedrick 2005) was 0.44, indicating that there is some differentiation between subpopulations. To reduce the effects of nearly identical isolates on local diversity estimates, reduced multilocus genotypes (MLGs) were defined using the IQTree maximum likelihood (ML) distance estimates using complete linkage clustering and a cutoff threshold of 0.1 (Table 1). All clusters other than 4 and 8 (the main WA population and the international isolates) were composed of a single MLG using this strategy. Cluster 4 comprised 89 MLGs (of 102 individuals) and cluster 8 comprised 14 MLGs (of 15 individuals). For each sampling location and year, a single individual of each MLG was selected for further comparison, referred to as the “clone-corrected” subset. A mantel test comparing the ML distance matrix with the distance matrix derived from the isolate sampling GPS coordinates indicated no significant correlation between genetic distance and geographic distance in the WA “clone-corrected” population (Mantel test, 999 replications, p-value = 0.381). Principal components analysis (PCA) of the clone corrected samples showed a clear separation of international isolates from those of WA in PC1 which explained 4.7% of the total variance, but no other principal components showed structure in the data correlated with sampling location or year (Fig S6 and S7).

Permutation tests of the r_d index of association indicated that all clusters except 1 and 7 were in linkage disequilibrium (999 replications, p-value < 0.05) (Table 1). Clusters 1 and 7 both contain only three members, so the test may be underpowered in those cases. Repeated tests for clusters 4 and 8 using the "clone corrected" subset were also significant, indicating that linkage disequilibrium was not associated with isolate clonality.

Comparative genomics across the local Western Australian *P. nodorum* population indicated telomeric or transposon-rich mutation 'hotspots'

Short variant mutation frequencies were observed to occur in "hotspots" throughout the SN15 genome, which were often, but not exclusively, telomeric (Fig 2, Table S8). The accessory chromosome 23 (AC23) was observed to have a higher overall SNP density compared to other chromosomes. Isolates WAC2813, WAC9178, WAC2810, WAC8635, WAC13405, WAC13418, WAC13447 (all from population cluster 6) all had very few SNPs relative to SN15, forming the inner blue circle present in Fig 2. Care was taken that certain biological and technical factors did not unduly influence our interpretation of SNP density at the whole-genome level. A region on chromosome 07 of between 140,979 bp and 623,833 bp, which was identified in a previous study (Bertazzoni et al. 2021) as a potential sequencing artifact exhibited an absence of SNPs in our analysis. Low SNP counts around the rDNA tandem repeat array located on the end of Chromosome 3 (Bertazzoni et al. 2021) and other areas that overlap repeat regions may have also been caused by read-alignment depth filtering rather than the absence of variants. Repeat-induced point mutation (RIP) is an important feature indicating 'hypermutation' compartments throughout fungal genomes (Hane et al. 2015). The ratio of RIP-like dinucleotide changes over all transition SNPs across the pan-genome relative to the SN15 reference genome indicated that RIP-like mutations are over-represented and also tend to be localised in hotspots (Fig 3). Hotspots of RIP-like mutation tended to co-locate with regions rich in transposable elements in the SN15 genome, though there are several regions that are enriched for RIP-like mutations for a small group of isolates.

Comparative genomics across the WA *P. nodorum* pan-genome

The average assembly size for the 156 WA *Parastagonospora nodorum* isolates was 37.8 Mb, with a median N50 of 17 and a median L50 and NG50 of 793431 and 783556 (Table S5).

Mitochondrial assemblies produced between 1 and 3 contigs in all cases, with a median size of 49591 bp. A common ~1000bp repeated region was observed in the mitochondrial assemblies, which appeared to be the cause of the fragmented assemblies (data not shown). The WA isolates were predicted to be highly complete with a median number of genes predicted by Genemark of 13037, with average completeness estimated via BUSCO at 98.94%, only one isolate (15FG111) had completeness estimated below 98%.

To identify potential regions of presence-absence variation (PAV), the genome assemblies of this study and previous studies (Richards et al. 2018, Phan et al. 2020) (Table S1) were aligned to the SN15 reference assembly (Bertazzoni et al. 2021). In comparison to the SN15 reference assembly, the majority of the SN15 genome sequence was conserved with resequenced isolate assemblies, with small regions of PAV tending to be observed at telomere ends or large internal repeat regions (Fig 4; Table S8). In addition to being missing in isolate SN79 (Richards et al. 2018), the accessory chromosome 23 was wholly absent in isolate 'Northam_Magenta' and partially absent in isolates 16FG160-162, 16FG163_2, 16FG164-171, and WAC13403 (Fig 4). We observed large duplications of genomic regions in some isolates (Fig 4). On SN15 chromosome 19 there was a large duplication of a region between 850 kb and 1 Mb in length in isolates WAC13404, WAC13075, and WAC13525. The first 200 kb was duplicated in isolate Meck8 relative to SN15 chromosome 22. Isolate WAC13631 had a large duplication relative to SN15 chromosome 12, of between 750 kb and 1.1 Mb.

Genes were predicted in all genome assemblies (including previously published isolates, Table S1), which resulted in a median gene count of 18294 across WA isolates, with a minimum of 17633 in isolate SN79 and a maximum of 19125 in isolate RSID03 (Table S6 and S7). The median length of coding domain sequences (CDSs) was 894 bp and was 53 bp for introns. The median BUSCO gene completeness was 3135 or 99.3%, with a median of 16 fragmented and 3 missing loci. Orthology clustering of predicted protein products from all *P. nodorum* isolates (including non-WA isolates) produced 34381 `orthogroups', 14098 of which were core to the population (13628 single copy and 470 multi-copy), and 11460 were dispensable (10043 single copy, 1417 multi-copy) (Table S9). An additional 8823 singleton groups were identified (8490 single copy, 333 multi-copy) which were only observed in a single isolate. To detect orthogroups with any members potentially under positive selection at any site, dN/dS branch site tests were run for all non-singleton orthogroups using the BUSTED algorithm in HyPhy (Pond et al. 2005). This identified 5306 orthogroups that were undergoing diversifying selection at any point with p-

values < 0.01. Of these, 732 orthogroups had more than 20% of sequences within the orthogroup predicted to be subject to positive selection.

Multiple codon alignment of the coding sequences of the three known effector loci *ToxA*, *Tox1*, and *Tox3* (Data S10) indicated the occurrence of non-synonymous and RIP-like mutations in these loci. The *Tox1* orthogroup (SNOO_20078A) was absent in isolates RSID36, RSID37 and RSID39 (Table S9) and was present as a single copy in all other isolates, or as a C-terminal truncated version in WAC13443 and SN79. Some branches of the orthogroup were predicted to be under positive selection (HyPhy BUSTED test, p-value >= 0.0008), and three codons showed significant position-specific positive selection (HyPhy FUBAR test, posterior probability > 0.90) at alignment codons 108 (GAC↔TCC; p=0.9194), 113 (ACC↔CCC; 0.9296), and 117 (GCA↔CAA; 0.9892). The alignment variants at T113P and R117[V,Q] are restricted to WA isolates, while the variant at D108S is restricted to a subset of the international isolates, including SN4. Overall, 13 distinct AA and nucleotide CDS sequences were detected in SNOO_20078A. The *Tox3* orthogroup (SNOO_08981AB) was present in 160 isolates, but absent in SN79, SN2000, and 8 of the 16 remaining non-Australian isolates. SNOO_08981AB was not predicted to be under positive selection (HyPhy BUSTED, p-value=0.05), and no specific positions were detected to be under positive selection using HyPhy FUBAR. Five distinct Tox3 codon sequences were observed resulting in two distinct AA sequences, with 28 WA isolates (including all isolates from population cluster 9) and one Swedish isolate (RSID28) possessing 3 mutations resulting in the codon changes N78D (AAT↔GAT), R102L (CTA↔CGA), and D104E (GAA↔GAT), with the first appearing to be RIP-like. The *ToxA* orthogroup (SNOO_16571A) was present in most isolates but absent in one WA isolate (201FG209), and 11 international isolates, including SN79. The *ToxA* orthogroup was not predicted to be under positive selection by HyPhy BUSTED, and no individual sites were predicted to be under positive selection by HyPhy FUBAR. There were non-synonymous mutations, I130V (ATT↔GTT) and E125D (GAA↔GAT), the former exclusive to WA isolates and the latter being

RIP-like and present in seven isolates, of which 2 were from WA. Five anomalous ToxA CDS sequences were observed, each with distinct AA sequences, however all of the predicted genes lacked a C-terminal region (which included the RGD motif) annotated in SN15, possibly indicating exon mis-annotation in these isolates.

Effector prediction using Predector (https://github.com/ccdmb/predector) identified 779 effector candidates in the SN15 reference isolate which were predicted to be secreted and with positive EffectorP 2 scores, and 1348 effector candidates with Predector scores greater than zero, of which 132 were homologous to known fungal effectors or had virulence associated Pfam domains. Across the entire pangenome, 2055 orthogroups were predicted to be secreted and have a positive EffectorP 2 prediction, 3398 orthogroups had members with a Predector effector score greater than zero. Of the predector candidates 997 were predicted to be secreted and +have a positive EffectorP 2 prediction, 145 contained effector homologues or virulence related Pfam domains, 411 had members significantly under positive selection, 55 were under positive selection in more than 20% of orthogroup sequences, 750 were accessory orthogroups, and 1405 were singleton orthogroups.

Orthogroups showed some PAV spanning large regions of the genome (Fig 5, Table S9). The largest of these was only present in 31 isolates and contained 385 orthogroups, comparable in gene number to AC23 which contains 218 predicted genes in SN15. Assembled scaffolds containing orthogroups in this PAV group were generally shorter than 200 kb, did not align to any chromosomes in the SN15 genome, but did align to scaffolds in other isolates with a high level of collinearity (Data S11).

Accessory regions and candidate effector loci are enriched in RIP-like mutations and unknown functions across the WA pan-genome

Statistically significant enrichment (two-tailed hypergeometric test, BH FDR corrected p-value < 0.05) of predicted protein functions (by gene ontology (GO) terms) were observed within various subsets of pan-genome orthogroups. The core pan-genome was enriched for 3509 GO terms generally associated with core functions including biosynthesis, cell cycle control, and transport (Table S11). Conversely, the accessory pan-genome was depleted in 1698 terms associated

with core functions. Similarly, singleton orthogroups (present in only one isolate) were depleted in 1708 GO terms associated with core functions, as were orthogroups not present in the SN15 reference isolate (2946 depleted). Multicopy subsets of the core, accessory, and singleton pan-genomes, and the subset of the accessory pan-genome containing between 20% and 80% of isolates showed similar patterns of enrichment and depletion as their respective supersets. Orthogroups where more than 20% of sequences were predicted to be positively selected were depleted in 139 GO terms relating to core functions (e.g. transport, metabolic processes, response to stimulus).

Genes of the SN15 reference isolate that were RIP-affected (above the RIP ratio 95th percentile, 0.432) were depleted in 54 core GO terms. AC23 contained two of the four genes in SN15 predicted to be involved in dehydroaustinol biosynthesis, but otherwise GO terms were all depleted. The large PAV group was depleted in 32 terms with general core functions. Overall, the enrichment tests above did not reveal any clear associations between GO terms and features within the genomic landscape. The majority of orthogroups (28767 of 34381) had no GO terms assigned. A complementary series of enrichment tests for a lack of GO terms ('no-GO') were performed using fishers exact tests with an uncorrected p-value threshold of 0.05. The core pan-genome was depleted for no-GO orthogroups, whereas the accessory and singleton pan-genome, positively selected orthogroups with more than 20% of sequences under selection, the PAV group, RIP-affected orthogroups and SN15 loci on AC23 were all significantly enriched no-GO orthogroups.

Enrichments tests were also performed for predicted secreted proteins and effector-like proteins (predicted secretion and EffectorP2). The accessory pan-genome, singleton pan-genome, orthogroups absent in SN15, and positively selected orthogroups were enriched for secreted proteins. However the core pan-genome and PAV groups were depleted in secreted proteins. Similarly the accessory pan-genome and positively-selected orthogroups were enriched in effector-like orthogroups, while the core and singleton pan-genomes were depleted.

To find effector candidates a representative member of each orthogroup for each distinct locus was selected (Table S10). For orthogroups with members in the reference isolate SN15, all distinct loci were included selecting the protein isoform with the closest sequence length to the average orthogroup length. Representative members of other orthogroups were selected by taking the member with the closest sequence length to the average orthogroup length, with a

preference for alternate reference isolates SN4, SN2000 and SN79. Orthogroups with a Predector score greater than zero, or with a signal peptide predicted by any method and an EffectorP 2 score greater than 0.5 were selected to be effector candidates. This identified 3579 candidate orthogroups, of which 788 and 1504 were in the accessory and singleton pangenomes, respectively. The WA isolates contained 1362 candidates (181 accessory) that were not predicted in the international isolates, of which 411 were restricted to the non-core populations (not cluster 4; 64 accessory). The core WA population (cluster 4) possessed 842 distinct candidates not present in other clusters (64 accessory), while clusters 6 (which includes SN15) and 8 (international) possessed 96 (1 accessory) and 375 (52 accessory) unique candidates. The reference isolates SN15, SN4, SN2000, and SN79 were missing 1732 candidate orthogroups (317 accessory).. There were 66 candidate orthogroups predicted to be under positive selection in at least 20% of orthogroup members, including a Tox3 homologue (SNOO_01097A). The large clusters of orthogroups with PAV identified in Fig 5 contained 18 candidate orthogroups. From these 3579 candidates, 1809 orthogroups with known functions or similarity to known effectors were selected (Table 2. Table S10).

Tox1 (SNOO_200780A, SNOO_304660A, SNOO_423420AB, SNOO_436740A, SNOO_531030), four Tox3 (SNOO_089810AB, SNOO_010970A, SNOO_438650A, SNOO_503200), and one ToxA (SNOO_165710A) homologous orthogroups were identified, including each of the original sequences from the SN15 isolate. Numerous other effector homologues were found, including 19 MoCDIP4 (Chen et al. 2013), 7 XYLA (Pollet et al. 2009, Sperschneider et al. 2015), CfTom1 (Pareja-Jaime et al. 2008, Ökmen et al. 2013), 2 FGL1 (Voigt et al. 2005), 2 AVR-Pita/AVR-Pita2 (Dai et al. 2010, Chuma et al. 2011), 2 Zt6 (Kettles et al. 2018), 2 HCE2/Ecp2 (Stergiopoulos et al. 2012), 2 NEP/NLP (Oome et al. 2014), 2 BEC2 (Schmidt et al. 2014) and 5 other CFEM domain containing proteins, 2 Cgfl (Fungalysin peptidase) (Sanz-Martín et al. 2016), and one each of BEC1019 (Zhang et al. 2019), NIS1 (Yoshino et al. 2012, Irieda et al. 2019), MoBas2 (Mosquera et al. 2009), MoCDIP1 (Chen et al. 2013), MoMSP1 (Wang et al. 2016), MoSPD5/MoBas4 (Mosquera et al. 2009, Sharpee et al. 2017), PevD1 (Bu et al. 2014), and ZtNIP2 (M'Barek et al. 2015). Other notable functions and families identified among these effector candidates include peptidases, nucleases, cupredoxins, CAP-superfamily proteins, Egh16-like virulence factors, Osmotin/Thaumatin-like proteins, Killer toxin KP4, tuberculosis necrotizing toxin, SnoaL-like/NTF2-like domain superfamily, RmlC-like cupin domain superfamily, TolB-like/major royal jelly protein, Ubiquitin and biotin related

436 functions, and WD40/Ankyrin/Kelch repeat-containing proteins. A single UstYa-like mycotoxin
437 biosynthesis protein, and several proteins related to metabolite biosynthesis or detoxification
438 were also found.

439

Discussion

The transition from the sequencing of a single or few reference genomes to larger populations has broadened the scope of comparative genomics of plant pathogens. This includes the identification of: additional accessory genome content missing from the reference isolate (Badet and Croll 2020); spatial distribution of virulence loci, and; region-specific selection pressures (Richards et al. 2019). To this end, we investigated the interplay between the population structure and genomic features relevant to plant pathogenicity, in a Western Australian population of *Parastagonospora nodorum*.

Population structure shows distinct regional sub-populations

Previously we have analysed the Western Australian *P. nodorum* population using SSR markers (Phan et al. 2020), and identified five distinct clusters of isolates. Two main clusters were proposed to represent a gradual change over time in response to wheat cultivar use, while the three remaining clusters were highly similar and were proposed to be clonally expanded populations. Interestingly, although the two core populations had a 1:1 ratio of mating type loci, the core population was observed to be in linkage disequilibrium, suggesting a predominantly asexually reproducing population. In contrast, this study indicated that the WA *P. nodorum* population is dominated by a single diverse main population, with seven satellite clusters that are highly similar. The fact that the core population was not split into two as previously observed may be explained by the marker type and number, the number of clusters selected to find, and the clustering method employed, where STRUCTURE (used in this study) explicitly models gene flow. The relative uncertainty of individual assignment to cluster 4 (the main population), suggests that there is some latent structure in the data, but this appears not to correspond to distinct reproductively isolated populations. In addition to the three satellite clusters identified by Phan *et al.* (Phan et al. 2020), the greater resolution gained by the use of many SNPs identified an additional 4 minor clusters, which were subdivided from the two previously identified core clusters (Fig S3). The relatively low diversity observed in these seven clusters suggests that these are very recent expansions or clonal subpopulations. Analysis of the index of association indicated that all but two small sub-populations are in linkage disequilibrium, suggesting that limited sexual reproduction is occurring in populations. It should be noted that the two exceptional population clusters (1 and 7) contained few isolates and their lack of linkage disequilibrium may be inaccurate. Linkage disequilibrium across WA *P. nodorum* sub-

populations was also reported by Phan *et al*. (Phan et al. 2020), but they observed that clusters P1 and P2 (corresponding to cluster 4 in this study) had a 1:1 mating type ratio which indicates the potential for sexual reproduction, and that cluster P5 (corresponding to cluster 9 in this study) was in linkage equilibrium. The finding that the international cluster is in linkage disequilibrium is also unexpected as it would imply that the global *P. nodorum* population is largely asexual, in conflict with numerous previous reports (Keller et al. 1997, Caten and Newton 2000, Murphy et al. 2000, Sommerhalder et al. 2006, Stukenbrock et al. 2006). Although the r_d values are significantly different from a random background, they are still relatively low so the population may be exhibiting a mixture of clonal and non-clonal reproduction. Alternatively, the permutation method of r_d may not be appropriate for samples with large numbers of SNPs in relatively high density (compared to low-throughput marker studies). Phan *et al*. (Phan et al. 2020) suggested that the non-core populations may be hybrids of local and internationally introduced *P. nodorum* isolates. This is not supported by the phylogenetic tree or population structure analysis reported in this study; however, STRUCTURE analysis indicated a cluster of six isolates from population 4 collected from the Northam and Dandaragan regions which had a high posterior probability of assignment to the international subpopulation, suggesting possible historic exchange of genetic material.

In the overall WA population there was no correlation observed between sampling location and genetic distance when nearly clonal isolates were excluded, suggesting that there are no geographic barriers to migration. Similarly, PCA only indicated an axis of variance separating international isolates from those from WA, with no other principal components showing association with sampling location or year (Fig S6 and S7). Long range wind dispersal of sexual ascospores has long been known to occur in the Western Australian *P. nodorum* population (Bathgate and Loughman 2001), though dispersal by infected seed is often reported internationally (Cunfer 1978, Cunfer 1998, Bennett et al. 2005). Both of these mechanisms may explain the lack of geography-dependent population structure observed in this study. Although seed borne dispersal is more likely if the population is mostly asexual, we were unable to find publications describing seed borne epidemics of *P. nodorum* in Australia.

The majority of isolates from the satellite clusters were collected from northern regions of the WA sampling area, predominantly Geraldton and Mingenew. Within the sampling zones presented in this study, the average rainfall in the south west regions is typically higher than in the dryer northern regions (http://www.bom.gov.au/climate/current/annual/wa/summary.shtml).

In addition to splash dispersal of secondary inoculum and a general positive correlation of rainfall with *P. nodorum* disease load (Solomon et al. 2006, Shaw et al. 2008), rain impacts can indirectly enable long-distance air travel (Kim et al. 2019), and may have contributed to the increased diversity of south-western regions. Similarly, high temperature during harvest time has been observed to be negatively correlated with *P. nodorum* disease load (Shaw et al. 2008), which may favour stronger populations in the southern regions. Numerous environmental factors can influence the lifecycle of *P. nodorum* which may explain these northern clonal sub-populations. However, the samples used in this study were not collected with population genetics analyses in mind, and an intentionally designed experiment may yet reveal the existence of similar structure in the other regions of the WA population. It appears that there is variance in the WA population, but this remains cryptic and is not explained by barriers to gene flow.

The presence of necrotrophic effector loci, or in some cases specific allele variants, is a direct determinant of crop disease outcomes in combination with the corresponding host sensitivity loci (Vleeshouwers and Oliver 2014). A US-based pan-genome study previously indicated alternate sets of candidate effector loci between two major *P. nodorum* sub-populations (Richards et al. 2019), highlighting the importance of region-specific genomic analysis and refinement of effector predictions in local isolates. The widespread surveillance of effector profiles within pathogen populations has great potential for crop disease management tailored to specific regions. In this WA-based study, low diversity sub-populations tended to have a conserved haplotype profile for the 3 known effector loci *ToxA*, *Tox1* and *Tox3* (Fig 1). In contrast sub-population cluster 5 exhibited notable diversity in its Tox1 effector haplotypes. Overall this study indicates the potential for resistant cultivars to be broadly recommended for growing across regions identified to have low diversity, but less reliably for regions with higher diversity. Given the extreme potential for genome plasticity in fungal genomes (McClintock 1941, Hane et al. 2011, Croll et al. 2013, Testa et al. 2016), it is encouraging that conserved effector haplotype profiles were observed in several cases. Identification of geographic regions exhibiting high variability of effector haplotype profiles within a narrow timeframe may also become an important element of crop disease monitoring in the future.

Pan-genome comparisons highlight regional diversity across the genomic landscape and effector contents

A previous comparison of *P. nodorum* isolates from the USA and Australia (Richards et al. 2018, Bertazzoni et al. 2021), indicated that the smallest chromosome (AC23) is an accessory chromosome with high levels of mutation, diversifying selection, and numerous gene duplications for redundant pathogenicity-related functions. Both AC23 and the region of chromosome 4 encoding the known effector gene *ToxA*, appeared to exhibit structural mutations that may be influenced by breakage-fusion bridge (BFB) formation. BFBs are hypothesised to be a driver of accessory chromosome formation and evolution (Croll et al. 2013, Bertazzoni et al. 2018) and of intrachromosomal recombination events that cumulatively lead to an inter-species conservation pattern termed “mesosynteny” (Hane et al. 2011). The largest duplications or absences in WA isolates relative to SN15 were predominantly located near telomeric regions or on AC23 (Fig 4). This is consistent with the known enrichment of structural rearrangement in subtelomeres (Hocher and Taddei 2020) and proposed prevalence of BFB-mediated rearrangement across the Dothideomycetes (Croll et al. 2013). Complete and partial absences of SN15 AC23 were observed in some Western Australian isolates, suggesting that large structural mutations are occurring in the field (Fig 4).

SNP density across the WA pan-genome was also consistently highest on AC23 (Fig 2) and near telomeres; however, several intrachromosomal mutation hotspots were also observed, where overall gene and repeat densities appeared relatively normal. The three known effector loci *ToxA*, *Tox1* and *Tox3* are all located at or near telomeres in SN15 (Bertazzoni et al. 2021), which also corresponded with SNP hotspots. Additionally a large orthogroup PAV cluster was observed in a subset of WA isolates, which may represent a previously undescribed accessory chromosome. Future long-read sequencing of these isolates may resolve the structure and history of these fragmented regions.

Overall, the variable genes and genome regions across the pan-genome (PAV and SNP) did not highlight any clear association with known gene functions. Indeed, the gene ontologies resource used in this study define function very broadly, and are biased towards conserved functions. Variable regions, including accessory, diversifying, repeat-rich and RIP-mutated, appeared to be bereft of known gene functions, but were conversely enriched in effector-like candidate loci. We observed 181 effector candidates that were absent in the international

isolates and present in more than one WA isolate, of which 68 were restricted to a single WA subpopulation. This suggests that WA may have a distinct pathogenicity gene profile; however, the number of non-Australian isolates used in study was relatively small, so further comparison with international isolates may find these candidates elsewhere. The large PAV cluster of orthogroups which may represent an accessory chromosome or large chromosomal PAV, contained 18 effector candidates, including two putative cupredoxins. Five Tox1 and four Tox3 homologous orthogroups in the pan-genome were found in different frequencies across the different populations. This suggests that these NEs may share a common origin but have since duplicated and diversified sufficiently that they were predicted as distinct orthogroups. Expansion and diversification of effectors within pathogen genomes appears to be a common phenomenon (de Guillen et al. 2015, Praz et al. 2017) in plant pathogens, and these homologues are strong effector candidates which may confer distinct phenotypes from their characterised homologues. Numerous homologues of effectors from other species were also identified, of which the necrotrophic effectors Zt6 and ZtNIP2 homologues are of particular interest to *P. nodorum*. Zt6 is a ribotoxin which cleaves non-self ribosomal sarcin-ricin loops in both wheat and microbial competitors (Kettles et al. 2018). ZtNIP1 induces light-dependent necrosis in wheat with differential responses between cultivars (M'Barek et al. 2015). Interestingly, numerous other homologues of avirulence elicitors and biotrophic effectors were also identified. Many of these have functions related to nutrient and sugar scavenging, but may still have a plausible virulence role in the necrotrophic *P. nodorum*. For example, numerous MoCDIP4 homologues were identified which induces cell death in non-host plants of *Magnaporthe oryzae* (Chen et al. 2013) and interferes with mitochondrial homeostasis, which in turn inhibits mitochondrially mediated resistance responses (Xu et al. 2020). The MoCDIP4-like effector candidate SNOG_01146 (SNOO_01146A) is significantly upregulated *in planta* and in a mutant lacking the effector-regulating PnPf2 transcription factor (Jones et al. 2019). Other effector-like orthogroups without fungal effector homologues but with potentially virulence-related functions were also identified. The putative aldose epimerase SNOO_61690 was one of the highest ranked candidates and only observed in isolate RSID03, but appears to be a highly truncated copy of SNOO_063350A which is present in all other isolates. In *Phytophthora sojae* the apoplastic aldose 1-epimerase AEP1 functions as a virulence factor by scavenging apoplastic aldose, and triggers cell death and pattern triggered immunity in *Nicotiana benthamiana* (Xu et al. 2021).

Comparative genomics across the WA pan-genome also indicated the prevalence of RIP-like mutations in variable regions, and was also associated with candidate effector loci. The presence of distinct genome wide patterns of RIP-like mutation between isolates would indicate that RIP has been actively occurring within a recent time frame. However RIP-like mutations did not correlate with diversifying selection observed across the whole genome, or even within highly ranked effector loci. RIP occurs during pre-meiosis, however, the observation of linkage disequilibrium suggests that the WA population may not be regularly undergoing sexual recombination. Although previous studies indicate *P. nodorum* has the potential for meiosis in WA (Murphy et al. 2000, Bathgate and Loughman 2001), it is yet to be determined if widespread RIP has only occurred in the past or if recent selection pressures have eliminated background isolate diversity. Investigations of the role of RIP in biotrophic and hemibiotrophic pathogens (Testa et al. 2016, Gervais et al. 2017) have indicated that RIP-mediated loss of a recognized avirulence effector may confer a selective advantage. We speculate that the nature of necrotrophic effectors with inverse gene-for-gene interactions with host sensitivity receptors (Fenton et al. 2009, Thrall et al. 2016) may conceal the full influence of RIP in necrotrophic effector diversification, as loss of function mutations are unlikely to be advantageous and would be selected against in the population. The remaining detectable RIP would be observable only for genome regions which do not significantly contribute a selective advantage. Nevertheless the *ToxA* locus resides in a large RIP hotspot on chromosome 4, and the confirmed effector loci *ToxA*, *Tox1* and *Tox3* retain a small number of non-synonymous RIP-like SNPs. The infrequent but constant potential for RIP to introduce potentially virulence enhancing mutations remains an important consideration for genome-guided disease risk assessment in necrotrophs.

Conclusion

Population-level pan-genome approaches are the next frontier of plant pathogen bioinformatics, which may eventually lead to affordable genome-based crop disease diagnostics and surveillance at a local level. Trends in pathogen genomics have begun to abandon intensive study of a single reference isolate, and are steadily progressing towards regionally-customised and data-driven assessments of pathogen gene-content, particularly with regards to effector genes (Richards et al. 2019, Badet and Croll 2020, Bertazzoni et al. 2021). In this study, we analyse a local Western Australian population of the wheat pathogen *Parastagonospora nodorum* and identify multiple genome features of relevance to this pathosystem. We observed an apparently high potential for genome adaptability, suggested by the presence of active RIP

633 and other mutations, but this was not readily observed to drive diversification of its three known
634 highly conserved necrotrophic effectors. Mutation hotspots were identified which were rich in
635 effector candidates and genes of unknown function, and often also classified as dispensable,
636 sub-telomeric or large repeat-rich regions. In a spatial context, we observed regional 'hot' and
637 'cold-spots' of population diversity, that may be linked to climatic factors affecting spore
638 dispersal. Across the local pan-genome, we observed the diversity of haplotype profiles of 3
639 known effector genes to be conserved in regions with lower overall diversity. A total of 3579
640 novel effector candidates were predicted across all isolates, with 2291 of these exhibiting PAV
641 across the genomes and 1362 restricted to WA isolates. Overall this study has progressively
642 improved bioinformatic resources for the *P. nodorum* pathogen, as well as advancing
643 approaches for the study of fungal pan-genomes with a view towards developing a region-
644 specific understanding of host-pathogen interactions.

645

Methods

DNA extraction and sequencing of Western Australian *P. nodorum* isolates

Genomic DNA of 141 previously described Western Australian *P. nodorum* isolates (Phan et al. 2020) were extracted (Xin and Chen 2012) and sequenced by the Australian Genome Research Facility (Melbourne, Australia) (Illumina HiSeq2500, TruSeq PCR-free, 125bp paired end (PE), 600 bp insert size) [NCBI BioProject: PRJNA612761] (Table S1). Genomic DNA of 17 new isolates and 14FG141 and Mur_S3 of the previous 141 were extracted using a Qiagen DNeasy Plant Mini kit (Venlo, Netherlands. Catalogue ID: 69104) and sequenced by Novogene (Beijing, China) (Illumina HiSeq2500, TruSeq PCR-free, 150bp PE, 350bp insert size). Pre-existing draft genomes of 15 international *P. nodorum* isolates (Syme et al. 2018) [NCBI BioProject: PRJNA476481] and chromosome-scale genome assemblies for the reference isolate SN15 (Bertazzoni et al. 2021), and for US isolates SN4, SN2000 and SN79-1087 [NCBI BioProject: PRJNA398070] (Richards et al. 2018) were also used.

Reads were trimmed for TruSeq universal adapters and low-quality using CutAdapt (v1.18) (2 passes, 3 trims/pass, terminal Phred score >2, average Phred score ≥5, length ≥50) (Martin 2011), and for contaminants (e.g. PhiX) using BBduk (v38.38, read kmer coverage of 0.7) (https://jgi.doe.gov/data-and-tools/bbtools/bb-tools-user-guide/bbduk-guide/), using the UniVec database (https://www.ncbi.nlm.nih.gov/tools/vecscreen/univec/) and the PhiX genome (NCBI RefSeq: NC_001422.1) (Sanger et al. 1978) as bait templates. Potential sample contaminants were searched for using Kraken (version 2.0.7) (Wood et al. 2019) searching against a database constructed from all NCBI Refseq bacterial, archaeal, protozoan, viral, and fungal genomes (downloaded: 2019-03-16), as well as the human GRCh38 genome (Wood and Salzberg 2014) (Table S2). The four published reference *P. nodorum* genomes (Richards et al. 2018, Bertazzoni et al. 2021) were also included as a positive set. Reads were aligned to the four reference *P. nodorum* genomes using BBmap (https://jgi.doe.gov/data-and-tools/bbtools/bb-tools-user-guide/bbmap-guide/, version 38.38) to evaluate insert size and completeness. Quality control statistics for each step were collected using FastQC version 0.11.8 (https://www.bioinformatics.babraham.ac.uk/projects/fastqc/), BBmap and Samtools (Li et al.

2009), and were collated using MultiQC (Ewels et al. 2016) (Data S1). Code for performing QC steps is available on GitHub at https://github.com/darcyabjones/qcflow (commit: e77715d).

Read alignment and variant calling

Short reads from all samples were aligned to the *P. nodorum* SN15 reference genome (Bertazzoni et al. 2021) using Stampy version 1.0.32 allowing multi-mapping reads (`--sensitive --substitutionrate=0.0001 --xa-max=3 --xa-max-discordant=10`) (Lunter and Goodson 2011). PCR duplicate reads in the aligned binary alignment map (BAM) files were marked using Picard version 2.18.29 (http://broadinstitute.github.io/picard/). Short variants were then predicted from the BAM files using GATK version 4.1.0.0 (McKenna et al. 2010, Poplin et al. 2018) and the following "bootstrapped" pipeline: 1) Call individual variants using `gatk HaplotypeCaller`. 2) Combine variants from all samples and run joint genotype prediction using `gatk GenotypeGVCFs`. 3) filter first pass variants with extreme statistics for each mutation type (snp, indel, or mixed) using `gatk VariantFiltration`. 4) Recalibrate the base quality scores in the BAM files using the predicted variants, using `gatk BaseRecalibrator` and `gatk ApplyBQSR`. 5) Steps 1-4 were repeated using the recalibrated BAM files until there was no difference in base quality score recalibration (BQSR) statistics between successive iterations. Filters applied at each bootstrap iteration are detailed in Table S3. An initial set of variants was found from the 140 isolates initially sequenced (excluding the resequenced SN15 isolate), using 5 bootstrap iterations to converge the BQSR scores. Nineteen additional sequenced isolates and 18 previously sequenced isolates (Syme et al. 2018), were then included in the analysis using the previously identified variant loci as starting points for two further bootstrap iterations including alignments from all isolates. Unfiltered variants were taken from the final bootstrap step and filtered more stringently. Individual genotype depth and genotype quality scores were visualised using the R (Team 2013) packages vcfR (Knaus and Grünwald 2017) and ggplot2 (Wickham 2016) to determine appropriate statistic cutoff thresholds, and were soft filtered using `gatk VariantFiltration` to have a minimum genotype "DP" statistic of 8 and minimum "GQ" score of 30. Variant locus "DP" and "MQ" score ranges to include were determined based on scores in non-repetitive regions visualised using vcfR `chromoplot`. Other variant loci statistics were visualised using ggplot2 to determine cutoff thresholds, and loci were filtered using `gatk VariantFiltration` separately for each variant type using the selected thresholds. All filtering parameters used during variant prediction are presented in table S3. Filtered variants with

effects on the translation of annotated genes (Bertazzoni et al. 2021) (i.e. non-synonymous or nonsense mutations) were identified using SnpEff (Cingolani et al. 2012).

Phylogeny estimation and population structure analysis

Single nucleotide polymorphisms (SNPs) for phylogenetic and population analyses were selected by excluding SNPs missing in more than 30% of isolates or with a SnpEff impact prediction of “HIGH” or “MODERATE”. To reduce the potential impact of small scale linkage disequilibrium, SNPs were selected using PLINK version 1.9 (Purcell et al. 2007) by taking SNPs with the highest minor allele frequency where two SNPs within 10 kb have an R^2 value greater than 0.6 (`--indep-pairwise 10 kb 1 0.60`). Resulting SNPs were then filtered to have a minimum non-major allele frequency of 0.05 using BCFtools (Li 2011) (`--min-af "0.05:nonmajor"`). SNPs were converted to a sequence alignment and the substitution model best fitting the data was predicted using ModelFinder in IQTree version 2.0.3 (`-st DNA -m "MF+ASC" -mset "GTR,JC,F81,K80,HKY,K81" -cmax 15 -rcluster 25 -safe`) (Kalyaanamoorthy et al. 2017). The best performing model was selected and used to construct a maximum likelihood tree using IQTree with 10000 UFBoot (Hoang et al. 2018) and 1000 SH-aLRT iterations (`-bb 10000 -bnni -alrt 1000 -st DNA`) (Minh et al. 2020). Phylogenetic trees were plotted using the R version 4.0.2 packages phytools v0.7-47 and ggtree v2.2.4 (Yu et al. 2017). Phylogenetic trees from this study and the tree published by Phan *et al*. (Phan et al. 2020) were visually compared using tanglegrams, implemented in the dendextend (version 1.14.0) package (Galili 2015).

Population structure was inferred from SNP data using STRUCTURE version 2.3.4 (Pritchard et al. 2000). To select an appropriate number of subpopulations (K) to model, STRUCTURE was run with 10000 replicate burn-in period and 20000 MCMC replicates for a range of values of K between 1 and 12, rerunning 8 times for each K to account for random starting points. The optimal value of K was selected using STRUCTURE HARVESTER (Earl and vonHoldt 2012) using the method described by Evanno *et al.* (Evanno et al. 2005). STRUCTURE was run using the selected value of K, using a 20000 replicate burn-in period and 100000 MCMC replications, running with 8 random seeds and selecting the run with the highest log probability of data given the model.

Population statistics were calculated and visualised using R version 4.0.2 packages: ade4 v1.7-15 (Thioulouse et al. 1997), adegenet v2.1.3 (Jombart 2008), poppr v2.8.6 (Kamvar et al. 2014), and vcfR v1.12.0 (Knaus and Grünwald 2017). The filtered SNP variants were imported into R and locus heterozygosity and G'_{st} (Hedrick 2005) scores were computed using vcfR. To account for effects near identical multilocus genotypes in population statistics calculations, the maximum likelihood (ML) distances from IQTree were used to identify MLGs that are highly similar and collapse them using poppr. For each cluster identified by STRUCTURE, the Shannon, Simpson, and inverse Simpson indices (Hurlbert 1971) were calculated, for both MLG collapsed and uncollapsed data using poppr. To test for linkage disequilibrium in population clusters, isolates from each population cluster were selected and a permutation test of r_d (a modification of I_A) (Agapow and Burt 2001) with 999 permutations was run for polymorphic loci within those isolates using poppr. To test for any correlation of geographic distance with phylogenetic distance in the WA isolate population, a Mantel test with 999 replications was performed using ade4 comparing ML distances from IQTree with euclidean distances of GPS coordinates from Australian clone corrected isolates with known sampling locations and distinct collapsed multilocus genotypes. Patterns of variance were assessed using principal component analysis (PCA) of the filtered SNPs from all isolates with distinct collapsed MLGs using the adegenet package.

Genome assembly

Overlapping 150 bp paired end reads from the WA isolates were stitched using BBmerge version 38.38 (Bushnell et al. 2017) using the strict mode, kmer size of 62 bp, allowing assembly extension up to 50 bp from the ends of reads (`rem` mode), and using error correction to assist merging (`ecct` option). Genomes were assembled using Spades version 3.13.0 (Bankevich et al. 2012) (parameters: `--careful --cov-cutoff auto`). Different kmers were used depending on input read length (Supp table 1) (125 bp PE samples: 21,31,51,71,81,101; 150 bp PE samples 31,51,71,81,101,127; 201FG217 [125 bp PE]: 21,31,51,71). Mitochondrial genomes (mtDNA) were assembled using Novoplasty version 2.7.2 (Dierckxsens et al. 2017), using the Sn15 mitochondrial genome assembly [NCBI RefSeq: EU053989.1] (Hane et al. 2007) as a seed sequence, and with kmers between 31 and 81 (table S5). The k-mer resulting in assemblies with the fewest number of contigs within an expected total assembly size of 47-52 Kb was manually selected and designated the mtDNA sequence of that isolate. Code for generating the mtDNA assemblies is available at https://github.com/darcyabjones/mitoflow.

Nuclear genome assemblies were then filtered for mtDNA sequences by aligning reads to assembled scaffolds using BBmap, and aligning mitochondrial scaffolds to assemblies using minimap2 git commit 371bc95 (Li 2018). Genomic scaffolds were considered to be mitochondrial if the alignment coverage with mitochondrial contigs was greater than 95%, and the median read depth was in the top 0.8% overall read depth. Some manual assignment of very short contigs near the threshold cutoffs was undertaken.

Genome assembly quality control statistics were collected using Quast version 5.0.2 (Gurevich et al. 2013), bbtools stats version 38.38 (https://jgi.doe.gov/data-and-tools/bbtools/bb-tools-user-guide/statistics-guide/), and KAT version 2.4.2 (Mapleson et al. 2017). Code for running post-assembly quality control and selection of mitochondrial scaffolds is available at https://github.com/darcyabjones/postasm (commit: c94c3b9).

Determining presence-absence variation relative to the SN15 reference isolate

Genome assemblies were aligned to the reference isolate SN15 (Bertazzoni et al. 2021), and to long-read assemblies for isolates SN4 [NCBI Assembly: GCA_002267005.1], SN2000 [NCBI Assembly: GCA_002267045.1], Sn79 [NCBI Assembly: GCA_002267025.1] using nucmer version 4.0.0beta2 (`--maxmatch`) (Marçais et al. 2018, Richards et al. 2018). Alignments were converted to BED format, from which alignment coverage was computed (`bedtools genomecov -bga`) and combined (`bedtools unionbedg`) using BEDTools version 2.28.0 into a bedgraph file (Quinlan and Hall 2010). Mean coverage in non-overlapping 50Kb windows of the genome visualised using the R package circlize (Gu et al. 2014).

Regions of PAV were extracted from the bedgraph using a custom python script (available at: https://github.com/darcyabjones/mumflow/blob/master/bin/find_pavs.py), and coverage blocks were converted to simple presence-absence values (0 or 1) by collapsing coverage count >= 1 to 1. Adjacent blocks with identical PAV values in all isolates were merged, and non-overlapping PAV blocks were also merged where for a set of 3 adjacent blocks, the outer 2 blocks had identical PAV values in all isolates and the centre block was <= 50bp. Code for running these steps is available at https://github.com/darcyabjones/mumflow.

Annotation of DNA repeats and non-protein coding gene features

Transposable elements (TEs) were predicted using a combination of tools: EAHelitron git commit c4c3dca (https://github.com/dontkme/EAHelitron), LTRharvest (Ellinghaus et al. 2008) and LTRdigest from genometools version 1.5.10 (Steinbiss et al. 2009), MiteFinder git commit 833754b (Hu et al. 2018), RepeatModeler version 1.0.11 (http://www.repeatmasker.org/RepeatModeler), and RepeatMasker version 4.0.9p2 (http://www.repeatmasker.org) using the species “Parastagonospora nodorum”. Putative TE protein coding regions in the genomes were identified using MMSeqs2 version 9-d36de (Steinegger and Söding 2017), searching protein profiles from selected Pfam families (table S6), GyDB families (Llorens et al. 2011), and a custom MSA database based on protein collections in TransposonPSI (http://transposonpsi.sourceforge.net/) and LTR_retriever (Ou and Jiang 2018) (available at: https://github.com/darcyabjones/pante/tree/master/data/proteins). Predicted TE sequences from EAHelitron, MiteFinder, RepeatModeler, and MMSeqs protein finding were combined and clustered using VSEARCH version 2.14.1 (Rognes et al. 2016) requiring cluster members to have >=70% identity to the cluster seed sequence (`--cluster_fast combined.fasta --id 0.90 --weak_id 0.7 --iddef 0 --qmask dust`). Clusters were filtered based on frequency and conservation across the population, requiring presence in >= 4 distinct genomic locations to be considered present in a genome, and requiring the cluster to be present in >= 20% of the total population. Filtered clusters were aligned using DECIPHER version 2.10.0 (Wright 2015), and classified into subtypes using RepeatClassifier (part of RepeatModeler), which was then used as a final customised library to map repeat locations for each assembly with a final round of RepeatMasker. Genes encoding rRNA and tRNA were predicted with RNAmmer version 1.2 (Lagesen et al. 2007) and tRNAscan-SE version 2.0.3 (Lowe and Chan 2016), respectively. These TE and non-coding RNA predictions were used to “soft-mask” genomes using BEDTools (Quinlan and Hall 2010). Code to run these steps is available at https://github.com/darcyabjones/pante/ (commit: 2de5d08).

Annotation of protein-coding genes

Proteins predicted from previous *P. nodorum* SN15 (Bertazzoni et al. 2021), SN4, and SN79 annotations (Richards et al. 2018) were aligned to each genome using Spaln version 2.3.3 (`spaln -KP -LS -M3 -O0 -Q7 -ya1 -yX -yL20 -XG20000`) (Iwata and Gotoh 2012).

Additionally all fungal proteins from the UniRef 50 database release 2019_08 (https://www.uniprot.org/uniref/, downloaded: 2019-10-29, query: 'taxonomy:"Fungi [4751]" AND identity:0.5') were aligned to genomes using Exonerate version 2.4.0 (`--querytype protein --targettype dna --model protein2genome --refine region --percent 70 --score 100 --geneseed 250 --bestn 2 --minintron 5 --maxintron 15000 --showtargetgff yes --showalignment no --showvulgar no`) (Guy St C and Ewan 2005) with pre-filtering by MMSeqs2 (`-e 0.00001 --min-length 10 --comp-bias-corr 1 --split-mode 1 --max-seqs 50 --mask 0 --orf-start-mode 1`) (Steinegger and Söding 2017). Published RNAseq data from *P. nodorum* SN15 *in vitro* and 3 days post infection of wheat leaves (Jones et al. 2019) (available in NCBI GEO project: GSE150493; NCBI SRA accessions: SRX8337785, SRX8337784, SRX8337783, SRX8337782, SRX8337777, SRX8337776, SRX8337775, and SRX8337774) were assembled using Trinity v2.8.4 (`--jaccard_clip --SS_lib_type FR`) (Grabherr et al. 2011) and aligned to genomes using Spaln version 2.3.3 (`-LS -O0 -Q7 -S3 -yX -ya1 -Tphaenodo -yS -XG 20000 -yL20`) (Iwata and Gotoh 2012), and GMAP version 2019-05-12 (Wu and Watanabe 2005). RNAseq reads were also aligned to all genomes using STAR version 2.7.0e (Dobin et al. 2013) and assembled into transcript annotations using StringTie version 1.3.6 (`--fr -m 150`) (Pertea et al. 2015).

Genes were initially predicted for each genome using multiple tools: PASA2 version 2.3.3 (`-T --MAX_INTRON_LENGTH 15000 --ALIGNERS blat --transcibed_is_aligned_oriented --TRANSDECODER --stringent_alignment_overlap 30.0`) (Haas et al. 2003), GeneMark-ET (`--soft_mask 100 --fungus`) (Lomsadze et al. 2014), CodingQuarry version 2.0 (including the unpublished "Pathogen Mode" with signal peptide predicted using SignalP version 5.0b (Testa et al. 2015, Armenteros et al. 2019), Augustus git commit 8b1b14a (independently for both `forward` and `backward` strands; `--hintsFile=hints.gff3 --strand=$(Dalman et al.) --allow_hinted_splicesites='gtag,gcag,atac,ctac' --softmasking=on --alternatives-from-evidence=true --min_intron_len=5`) (Stanke et al. 2008), and GeMoMa version 1.6.1 (transferring SN15 annotations only) (Keilwagen et al. 2018). Gene predictions using PASA2 used hints from assembled RNASeq transcripts aligned to the genomes with GMAP and BLAT. Augustus gene predictions used transcript alignments by GMAP, intron locations from STAR read alignments, and Spaln and protein alignments by Spaln as hints.

Pan-genomic gene sets may be prone to annotation errors in which orthologous loci are incorrectly annotated in some isolates, leading to false absences. To improve annotation

consistency between isolates, protein predictions from PASA, Augustus, and CodingQuarry from all isolates were clustered using MMSeqs2 (90% identity and 98% reciprocal coverage), and annotations corresponding to proteins from representative members of the clusters were transferred to all isolates using GeMoMa as described earlier. Annotations and alignments from Genemark-ET, CodingQuarry, Augustus, PASA, both GeMoMa configurations, Exonerate, Spaln protein and transcript alignments, and GMAP alignments were combined using EVidenceModeler (git commit 73350ce) (`--min_intron_len 5`) (Haas et al. 2008). Because EVidenceModeler does not support prediction of non-standard splice sites or overlapping genes in different strands, Augustus (with all hints and the same parameters described earlier) was used to predict additional genes in regions of the genomes with hints that didn't overlap the EvidenceModeler predicted genes on the same strand. Protein predictions were searched against AntiFam (Eberhardt et al. 2012) using HMMER version 3.2.1 (`--cut_ga`) and matches to pseudogenes were removed. Genes within the merged Augustus and EVidenceModeler gene sets were marked as "low confidence" if supported only by Spaln or GMAP transcript alignments, Exonerate protein alignments, or transfers of annotations between isolates performed via GeMoMa (excluding the initial set of genes transferred from curated SN15 annotations). In SN15, genes only supported by the above tools or Augustus were also marked as low-confidence. "Low-confidence" genes that overlapped other genes on either strand by more than 30% of their length were removed. We corrected errors in the CDS coordinates where phases of gene annotations may lead to incorrect translations in some downstream pipelines by searching against all proteins from other isolates without stop codons, and all Pezizomycota proteins from UniRef-90 (filter: 'taxonomy: "Pezizomycotina [147538]" AND identity:0.9'; downloaded: 2020-05-13) using blastx version 2.10.0 (`-strand plus -max_intron_length 300 -evalue 1e-5`) (Camacho et al. 2009). Genes with an in-phase BLAST match lacking internal stop codons were fixed and retained, genes with an out-of-phase BLAST match with internal stop codons were marked as pseudogenes, and those with no BLAST match and internal stops were discarded. Genes overlapping predicted rRNA genes by more than 50% of their length were also discarded, and genes with exons overlapping assembly gaps were split into multiple fragmented genes, where each fragmented annotation was >= 60 bp.

Gene prediction completeness was evaluated for each isolate using BUSCO version 3 (git commit 1554283) using the "pezizomycotina_odb9" dataset (Waterhouse et al. 2018), and additional statistics were collected by genometools version 1.5.10 (Gremme et al. 2013). The

updated SN15 annotations were compared to previously published gene annotation versions (Bertazzoni et al. 2021) using ParsEval/AEGeAn version 0.15.0 (Standage and Brendel 2012). The new SN15 annotations were identified using BEDTools, by excluding all new mRNA predictions overlapping original SN15 “A” and “B” mRNA annotations from (Bertazzoni et al. 2021) on the same strand >= 20% by length (`bedtools subtract -a new -b old -s -A -F 0.2`), and were designated as the “C” gene.

Orthology & positive selection

Orthology relationships for predicted proteins were predicted using Proteinortho version 6.0.30 (-singles -seflblast) (Lechner et al. 2011) with using Diamond version 2.0.8 (Buchfink et al. 2021). Alternative isoforms present in the SN15 annotations were included in the orthology finding. Orthologous clusters were assigned identifiers prefixed by ``SNOO'' (supplementary table S10), where clusters with members in isolate SN15 were assigned numbering corresponded to “SNOG” locus numbers (Bertazzoni et al. 2021) (Complete data: https://doi.org/10.6084/m9.figshare.12966971.v3). SNOO groups were also assigned alphabetical prefixes where one or more isoforms were present in SN15. For example “SNOO_434350AB” contains both *SNOG_434350* isoforms A and B, and “SNOO_033200A149040A” contains both SNOG_033200A and SNOG_149040A. Clusters without members in SN15 were assigned sequential numbers starting from 50,000. For the purpose of analysis of selection pressure, a representative SN15 isoform was selected for each SNOO orthogroup by selecting the isoform with the closest length to the mean sequence length of the orthogroup. Representative CDS sequences of SNOO orthogroups were codon-aligned using DECIPHER version 2.16.1 (Wright 2015), and gene trees were estimated using FastTree version 2.1.11 (Price et al. 2010). The SNOO orthogroup codon multiple sequence alignments and the gene trees were used to test for positive selection in the orthogroups using the BUSTED method in the HYPHY package version 2.5.15 (Pond et al. 2005, Murrell et al. 2015). A p-value threshold of 0.01 was used to determine positively selected SNOO orthogroups. Position specific positive selection tests were performed for the known effectors ToxA, Tox1, and Tox3 using the FUBAR method in the HYPHY package (Pond et al. 2005, Murrell et al. 2013).

For the purposes of PAV and pan-genomic comparisons, to account for alternate isoforms present across multiple orthogroups, temporary “locus groups” were constructed by combining

orthogroups that share common loci. Copy numbers of locus groups were calculated for each isolate as the number of distinct loci. Large PAV regions were identified by heriarchically clustering locus groups and samples by copy number using UPGMA clustering and the manhattan distance metric for orthogroups and 1 - Pearson's correlation coefficient as a distance metric for isolates. Manually-selected clusters of locus groups showing PAV were aligned to the SN15 genome where possible using MashMap v2.0 (-s 500 –filter_mode none) (Jain et al. 2018). Orthogroups were designated as "core" if all isolates contained at least one member in the parent locus group, as "accessory" if more than one isolate but not all isolates had at least one member in the locus group, and as "singleton" if the locus group was only detected in a single isolate. Additionally, locus groups were designated as "multicopy" if any isolate had more than one member.

Functional analysis & effector candidate prediction

Predicted whole protein functions were found by searching the Swiss-Prot database version 2020_02 (Bairoch and Apweiler 2000) using MMSeqs2 version 11-e1a1c (`--start-sens 3 -s 7.5 --sens-steps 3 -a`) (Steinegger and Söding 2017). Matches were considered reliable for functional annotation if they covered >= 70% of both sequences, with >=60% sequence identity, and an e-value < 1e-10. Functional domains were predicted using InterProScan (Jones et al. 2014, Mitchell et al. 2019). Additionally, GO-terms and predicted product names were predicted using the web-servers of PANNZER (Koskinen et al. 2015) and eggNOG-Mapper (Huerta-Cepas et al. 2017). GO-term predictions from InterProScan, PANNZER, and eggNOG-Mapper were combined and filtered to exclude terms in the GO do_not_annotate "anti-slim" set (available at: http://geneontology.org/docs/download-ontology, downloaded: 2020-05-15) to remove uninformative terms, forming the final GO-term set for the predicted proteomes.

Effector-like sequences were predicted using the Predector pipeline (https://github.com/ccdmb/predector, version: 0.1.0-alpha), which incorporates several software analyses including SignalP versions 3.0, 4.1g, 5.0b (Armenteros et al. 2019), DeepSig (Savojardo et al. 2018), TargetP version 2.0 (Armenteros et al. 2019), DeepLoc version 1.0 (Almagro Armenteros et al. 2017), TMHMM version 2.0c (Krogh et al. 2001), Phobius version 1.01 (Käll et al. 2004), EffectorP versions 1 and 2 (Sperschneider et al. 2016, Sperschneider et al. 2018), ApoplastP version 1 (Sperschneider et al. 2018), LOCALIZER (Sperschneider et al. 2017), homology searches against dbCAN version 8 using HMMER version 3.3 (Yin et al. 2012,

Mistry et al. 2013), and sequence matches against PHI-base version 4.9 (Urban et al. 2020) using MMSeqs2 version 11.e1a1c (Steinegger and Söding 2017).
Information from Predector, InterProScan, Pannzer, eggNOG-mapper, positive selection and orthogroup analyses were combined into a single table (summarised in table S10. Complete data available at https://doi.org/10.6084/m9.figshare.12966971.v3).

Enriched and depleted GO terms were detected for core, accessory, and singleton orthogroups (and their multicopy subsets), accessory orthogroups contained in between 20% and 80% of isolates, orthogroups predicted to be under positive selection anywhere in the gene tree and with more than 20% of members, for orthogroups not found in SN15, manually selected clusters of orthogroups identified from hierarchical clustering (Table S9), *P. nodorum* Sn15 genes on accessory chromosome 23, and *P. nodorum* Sn15 genes with a ratio of RIP-like mutations over transitions within 1000 bp of the gene over the 95th percentile, using two-tailed hypergeometric tests implemented in the GOATOOLS version 1.0.6 (Klopfenstein et al. 2018). For each of these sets, two-tailed hypergeometric/Fisher's exact tests were also used to test for enrichment of genes lacking any GO term assignments, genes annotated as secreted by the Predector pipeline, and genes annotated as secreted and with a positive EffectorP 2 prediction using the SciPy Python package (Virtanen et al. 2020).

Data availability

All sequencing data, genomes and annotations generated are available under NCBI Bioproject: PRJNA612761. Gene annotations for isolates SN2000, SN4, and SN79, as well as short variant predictions relative to SN15 are deposited online at (https://doi.org/10.6084/m9.figshare.13340975). Complete functional annotations, orthogroup assignments, CDS alignments and trees, and positive selection tests are available online at (https://doi.org/10.6084/m9.figshare.12966971.v3}. Supplementary material is also available online at (https://doi.org/10.6084/m9.figshare.13325915.v2).

Figure Legends

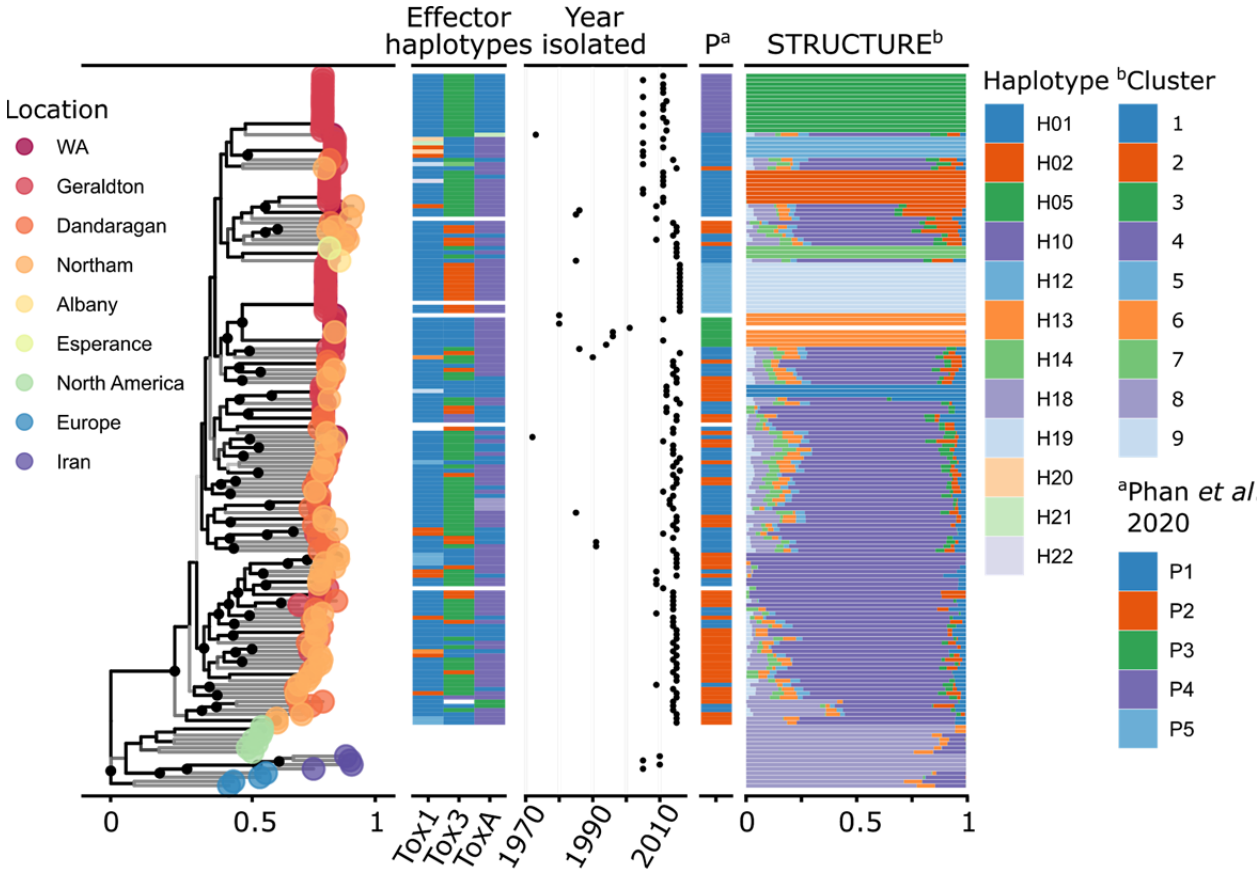

Fig 1. The structure and features of the Western Australian (WA) *Parastagonospora nodorum* population. The tree on the left shows the predicted phylogeny of WA and internationally-sampled *P. nodorum* isolates, with colours corresponding to sampling regions, summarised from Fig S1. Dots on the tree indicate where clades have >= 95% UFBoot confidence, and clade shade indicates SH-aLRT scores, with black indicating high support. Effector haplotype profiles for three confirmed effector loci are shown based on data from Phan *et al.* (Phan et al. 2020). A haplotype with white indicates that the isolate has not been haplotyped, or was unable to be amplified by PCR. On the right shows the results of population structure analysis, with colours indicating discrete population clusters, and the relative size of the bars indicating posterior probability of an isolate belonging to that cluster. The section indicated as “P” shows the clusters assigned to that isolate by the SSR study from Phan *et al*. (Phan et al. 2020), where white indicates isolates that were not present in that study

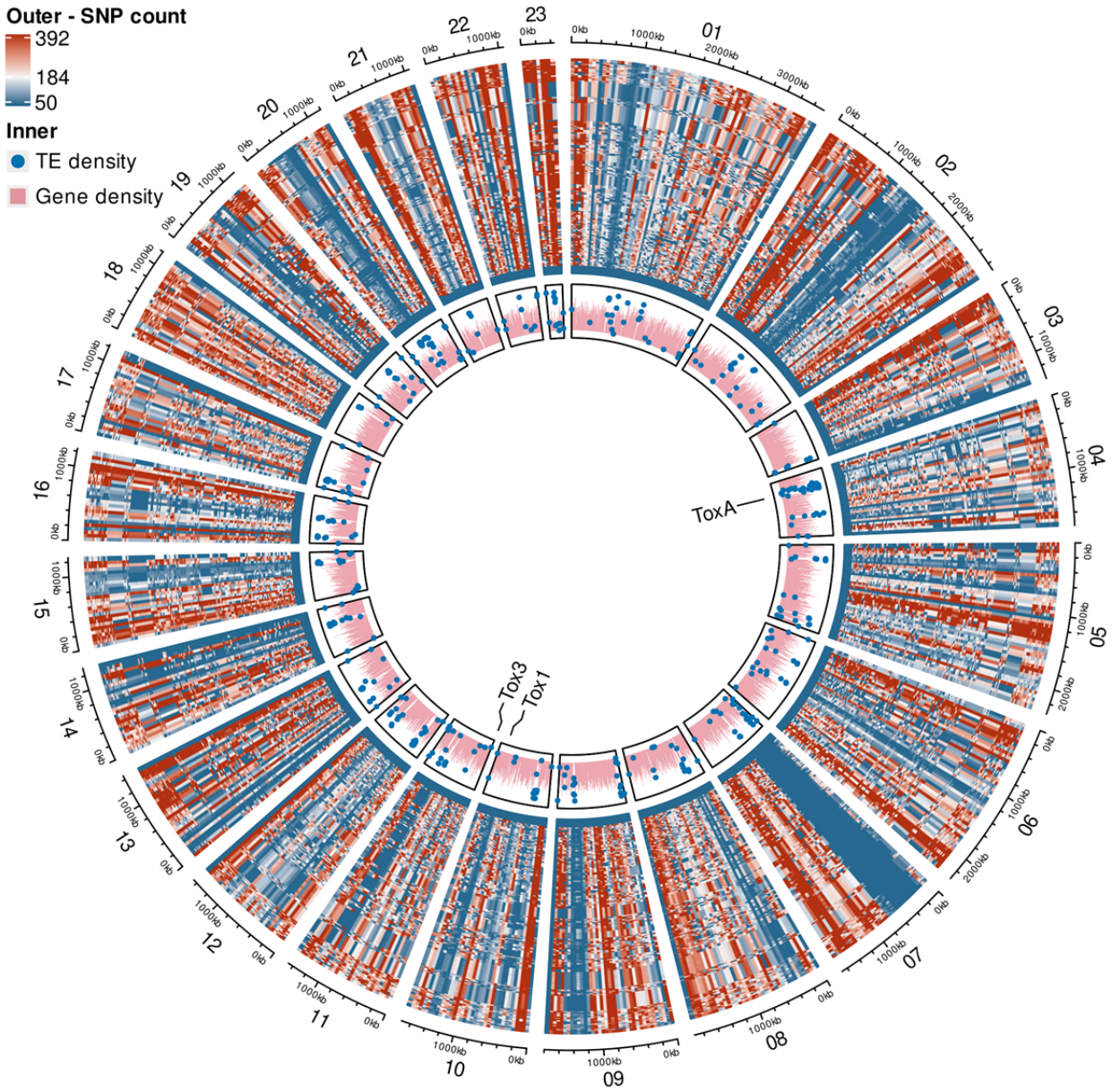

Fig 2. A circos plot showing SNP density over each of the 23 chromosomes in the SN15 genome assembly. The innermost track shows the proportion of bases covered by genes (CDS features, red) and transposable elements (TE, blue dots) in non-overlapping 10kb windows. For TEs, windows with TE base coverage less than 10% are not plotted. The heatmap shows SNP counts in 50 kb non-overlapping windows for each of the Western Australian isolates in the outer track (Table S8), with the colour scale boundaries set by the 10th, 50th, and 90th percentiles (50, 184, and 392, respectively).

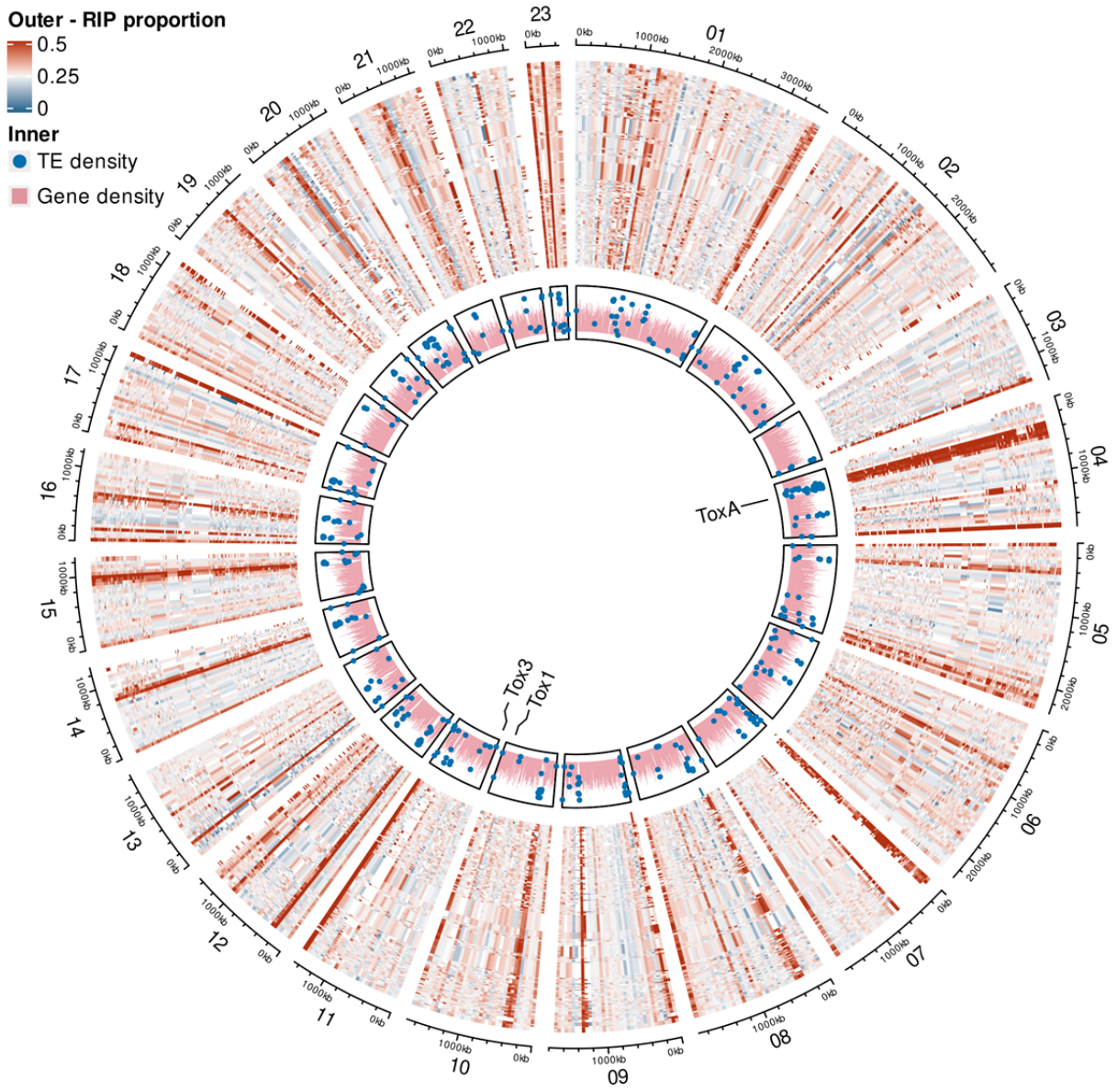

Fig 3. A circos plot showing the proportion of RIP-like (CA↔TA or TG↔TA) mutations over transition (C↔T or G↔A) mutations for each of the 23 chromosomes in the SN15 genome assembly. The innermost track shows the proportion of bases covered by genes (CDS features) and transposable elements (TE) in 10kb non-overlapping windows. Windows with TE base coverage less than 10% are not plotted. The heatmap in the outermost track shows the proportion of RIP-like mutations over the number of transition mutations in 50 kb non-overlapping windows for each isolate (Table S8). Windows with fewer than 20 SNPs are plotted in white to avoid high ratios caused by a small number of RIP-like mutations. By chance, 25% of transition mutations would be expected to be part of a RIP-like dinucleotide pair change.

1022

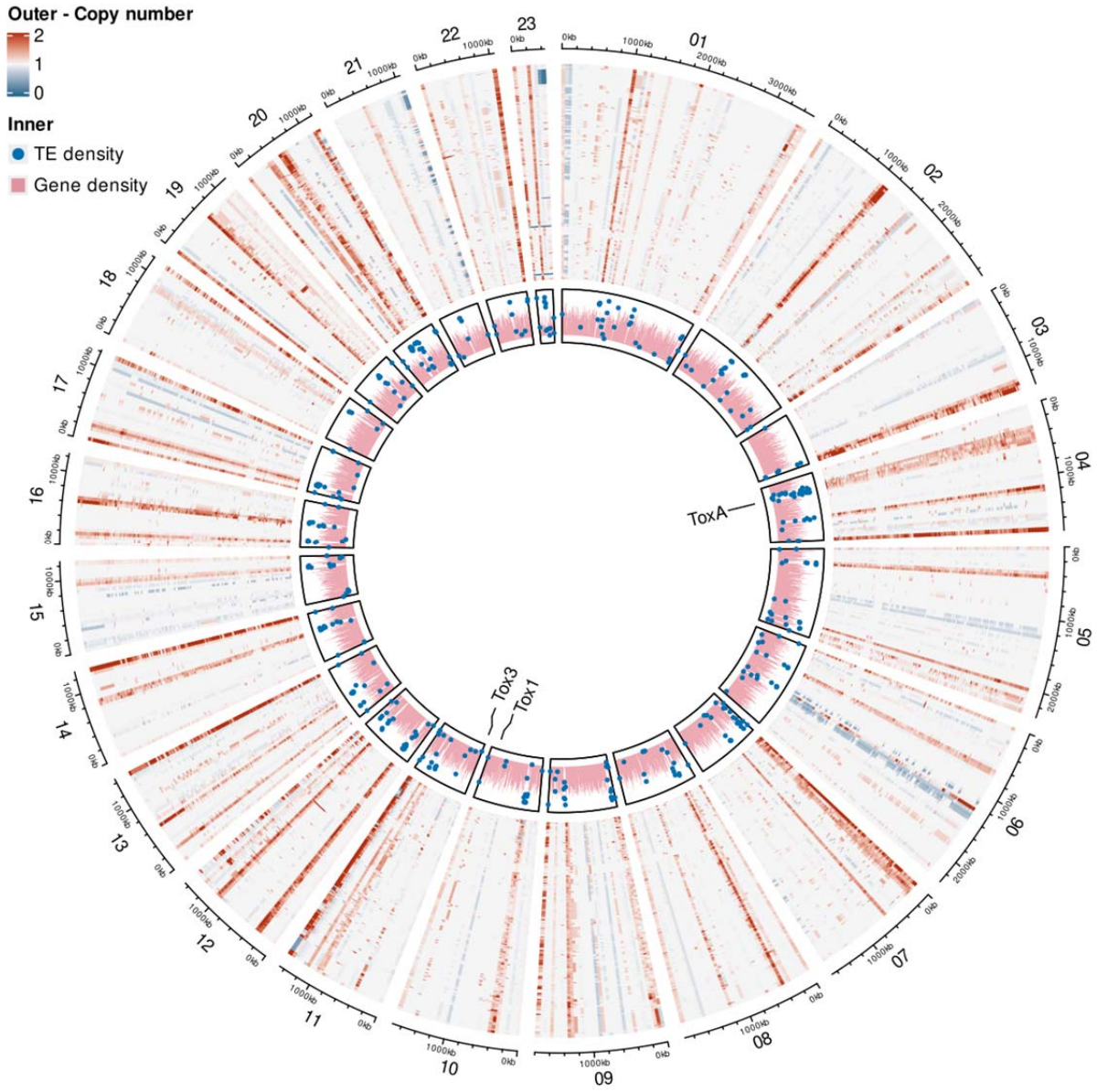

1023

1024 **Fig 4**. A circos plot showing each *Parastagonospora nodorum* genome assembly alignment
1025 coverage for each of the 23 chromosomes in *P. nodorum* SN15. The innermost track shows the
1026 proportion of bases covered by genes (CDS features) and transposable elements (TE) in 10kb
1027 non-overlapping windows. Windows with TE base coverage less than 10% are not plotted. The
1028 heatmap on the outside track shows average alignment coverage of each isolate genome
1029 assembly to SN15 in 50 kb non-overlapping windows (Table S8).

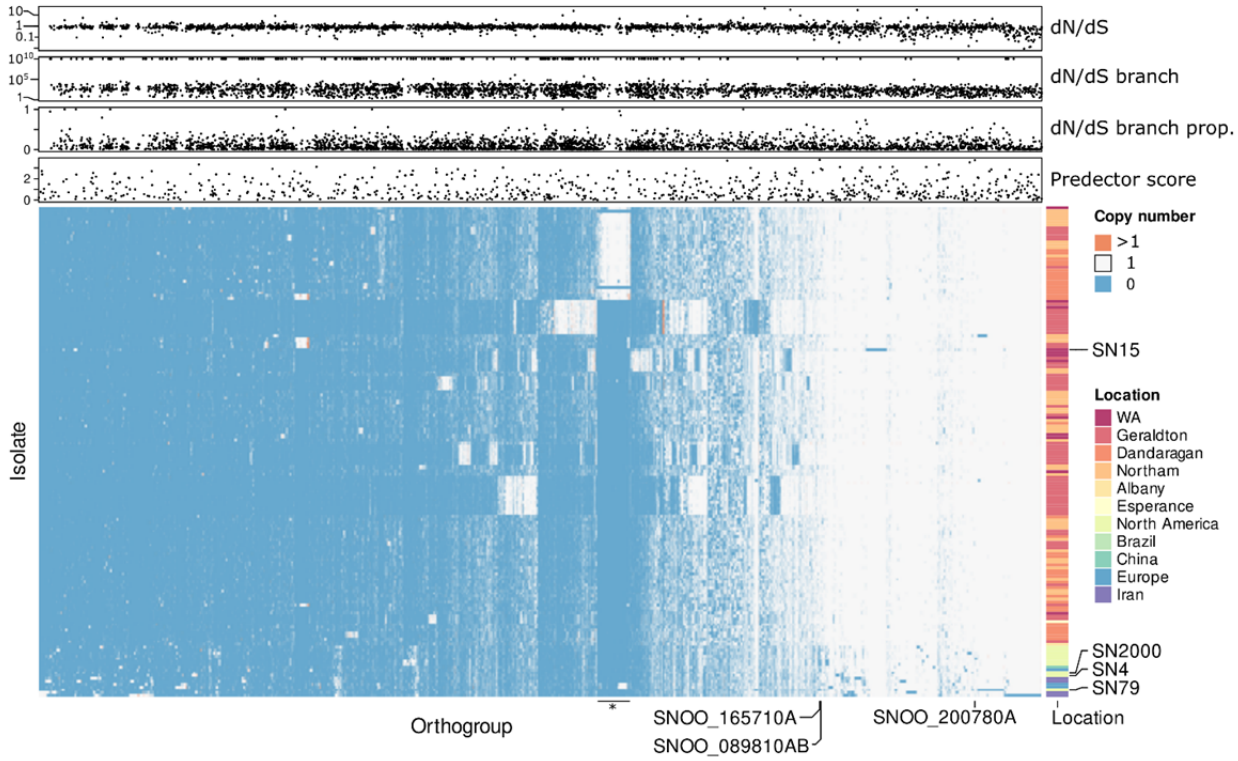

Fig 5. Dispensable and multi-copy orthogroups for each isolate in the *P. nodorum* pan-genome. "Orthogroups" is used as a general term to cover both orthologues and paralogues, which have not been separated here. Heatmap rows represent each *P. nodorum* isolate, and columns indicate each of the dispensable or multicopy orthogroups. Heatmap colour indicates the number of copies of an orthogroup each isolate has. Orthogroups absent (blue), present with single copy genes (white) and present with multicopy genes (orange) are shown. The columns of orthogroups containing ToxA (SNOO_16571A), Tox3 (SNOO_08981AB), and Tox1 (SNOO_20078A) are indicated. Locations that isolates were collected from are indicated on the right hand side colour bar. The rows corresponding to reference *P. nodorum* isolates are indicated. The top 3 scatter plots indicate orthogroups with any members with significant positive selection tests ($p < 0.01$). "dN/dS" indicates the overall dN/dS for the whole orthogroup. "dN/dS branch" indicates the dN/dS at the branch predicted to be under the highest selection. "dN/dS branch prop" indicates the proportion of sequences in the orthogroup predicted to be under positive selection. "Predector score" indicates where the highest scoring member of an orthogroup was greater than 0.

Tables

Table 1 Population diversity statistics based on 45,194 SNP variant loci (44,532 biallelic) from the *P. nodorum* population. Isolates are assigned to populations based on the STRUCTURE cluster with the highest posterior probability. No isolates had the same SNP profile, so multilocus genotypes (MLGs) were defined as having a genetic distance (estimated by IQTree) less than 0.1. The column "# loci" indicates the number of loci within a subpopulation that were variable and had no missing genotypes. The mean locus Simpson's index (Mean λ. AKA expected heterozygosity) is calculated for every locus under analysis, for a biallelic SNP in a haploid organism the maximum possible value is 0.5. The Simpson's index (λ), Stoddart-Taylor's index (G), and Shannon's diversity (H) are calculated based on MLGs. The index of association (IA) and it's normalised form ($\bar{r}d$) indicate linkage disequilibrium in each population cluster, and was calculated only on variant loci with no missing data (# loci) within each cluster. rd p-values indicate the result of a permutation test (999 permutations) for higher rd than would be expected by random allele distribution across isolates.

	# isolates	# MLG	# loci	F_{ST}	Mean λ	λ	G	H	I_A	$\bar{r}_d$	$\bar{r}_d$ p-value
Cluster 1	3	1	155	0.99	0.002	0	1	0	0.11	7e-3	0.325
Cluster 2	8	1	149	0.99	0.002	0	1	0	3.77	0.03	0.001
Cluster 3	14	1	156	0.99	0.003	0	1	0	0.58	0.004	0.026
Cluster 4	102	89	10353	0.05	0.311	0.99	81.28	4.45	1.53	0.006	0.001
Cluster 5	5	1	114	0.99	0.002	0	1	0	2.38	0.021	0.001
Cluster 6	7	1	33	1.0	0.001	0	1	0	1.27	0.040	0.021
Cluster 7	3	1	114	0.99	0.001	0	1	0	-0.03	-2e-3	0.363
Cluster 8	15	14	6695	0.0	0.314	0.92	13.24	2.62	11.85	0.013	0.001
Cluster 9	12	1	87	1.0	0.001	0	1	0	0.54	0.006	0.048
Total	169	110	45194		0.320						

Table 2 Selected effector candidate orthogroups with functional annotations in the *P. nodorum* pangenome. Of the 1908 effector candidates with functional predictions, this table includes all candidates with effector homologues and a Predector score > 1, the 5 top ranking (by Predector) orthogroups that were under positive selection, the top 5 candidates specifc to any populations identifed by structure, and the top 5 candidates restricted to Western Australian or non-core (satellite) WA population clusters. Population cluster 8 includes the international isolates, and cluster 4 represents the core WA cluster. For each candidate orthogroup SN15 members were selected as representatives, or in the case of orthogroups absent in SN15 the member with the highest Predector score. Membership of PAV clusters shown in Fig 5 is indicated by the corresponding number, where applicable. Products in bold show where a candidate matched a known necrotrophic or avirulence effector. All orthogroup candidates presented here have a signal peptide predicted by at least one method, and none any predicted transmembrane (TM) domains.

						Population cluster																
orthogroup	**Pangenome**	**SN15**	**SN4**	**SN2000**	**SN79**	**1**	**2**	**3**	**4**	**5**	**6**	**7**	**8**	**9**	**product**	**dN/dS**	**Predector**	**EffectorP1**	**EffectorP2**	**ApoplastP**	**LOCALIZER**	**Length**
SNOO_047630A	C	1	1	1	1	3	8	14	102	5	8	3	18	12	chitin binding domain-containing protein	0	3.94	1	0.98	0.88		30
SNOO_616900	S	0	0	0	0	0	0	0	0	0	0	0	1	0	aldose epimerase	0	3.79	0.96	0.93	0.8		20
SNOO_165710A	**A**	**1**	**1**	**1**	**0**	**3**	**8**	**14**	**101**	**5**	**8**	**3**	**7**	**12**	**ToxA**	**0**	**3.76**	**1**	**0.95**	**0.48**	**C**	**178**
SNOO_200780A	**A**	**1**	**1**	**1**	**1**	**3**	**8**	**14**	**102**	**5**	**8**	**3**	**15**	**12**	**Tox1**	**0**	**3.73**	**1**	**0.97**	**0.64**		**117**
SNOO_576590	S	0	0	0	0	0	0	0	0	0	0	0	2	0	Gamma-crystallin-like family protein	0	3.32	1	0.94	0.84		118
SNOO_423420AB	A	1	0	0	0	0	1	14	54	5	8	3	4	0	Tox1-like protein	0	3.08	1	0.95	0.72		124
SNOO_109810A	C	1	1	1	1	3	8	14	102	5	8	3	18	12	MoCDIP4-like glucanase	0	3.04	0.83	0.82	0.73		233
SNOO_638140	S	0	0	0	0	0	0	0	0	0	0	0	1	0	glycoside hydrolase	0	2.93	0.99	0.85	0.76		110
SNOO_107590A	A	1	1	1	1	3	8	14	102	5	8	3	17	12	FgXYLA-like xylanase	0	2.93	0.44	0.82	0.8		241
SNOO_160630A	C	1	1	1	1	3	8	14	102	5	8	3	18	12	Zt6-like endoribonuclease	0	2.92	0.99	0.88	0.56		174
SNOO_522100	A	0	0	0	0	3	0	1	26	0	0	0	0	0	RWD-like superfamily protein	0	2.88	1	0.78	0.26		108
SNOO_616750	S	0	0	0	0	0	0	0	0	0	0	0	1	0	glycoside hydrolase	0	2.82	0.93	0.83	0.86		159
SNOO_304660A	C	1	1	1	1	3	8	15	102	5	8	3	18	12	Tox1-like protein	0	2.81	1	0.93	0.5		84
SNOO_089810AB	**A**	**1**	**1**	**0**	**0**	**3**	**8**	**14**	**99**	**5**	**8**	**3**	**8**	**12**	**Tox3**	**0**	**2.78**	**0.87**	**0.89**	**0.27**		**230**
SNOO_568060	A	0	0	0	0	0	0	0	0	0	0	0	2	0	arabinofuranosidase	0	2.71	0.99	0.88	0.7		168
SNOO_531830	A	0	0	0	0	0	0	0	15	0	0	0	0	0	RWD-like superfamily protein	0	2.71	1	0.74	0.2		108
SNOO_128450A	A	1	1	1	1	3	8	14	101	5	8	3	17	12	FgXYLA-like xylanase	0	2.63	0.04	0.79	0.88		230
SNOO_137220A	C	1	1	1	1	3	8	14	102	5	8	3	18	12	MoMSP1-like cerato-platanin	0	2.58	0.65	0.69	0.91		136

SNOO_121270A	C	1	1	1	1	3	8	15	102	5	8	3	18	12	MoCDIP4-like glucanase	0	2.56	0.2	0.68	0.78		232	2
SNOO_096500A	C	1	1	1	1	3	8	14	102	5	8	3	18	12	FgXYLA-like xylanase	0	2.54	0.06	0.64	0.87		221	2
SNOO_427940A436170A	A	1	0	0	0	3	0	13	51	5	17	0	0	12	RWD-like superfamily protein	1	2.54	1	0.69	0.18		107	1
SNOO_120370A	C	1	1	1	1	3	8	14	102	5	8	3	18	12	MoCDIP4-like glucanase	0	2.5	0.29	0.73	0.82		246	4
SNOO_436740A	C	1	1	1	1	3	8	14	102	5	8	3	18	12	Tox1-like protein	0	2.48	1	0.94	0.76		79	8
SNOO_138880A	C	1	1	1	1	3	8	14	102	5	8	3	18	12	MoBas5/MoSPD5-like protein	0	2.44	1	0.91	0.36		106	6
SNOO_531030	A	0	0	0	0	0	1	2	8	0	0	0	3	0	Tox1-like protein	0	2.43	1	0.89	0.33	N	128	7
SNOO_527620	A	0	0	0	0	0	0	0	12	5	0	0	0	0	Major royal jelly family protein	0	2.38	0.9	0.78	0.65		213	0
SNOO_573060	A	0	0	0	0	0	0	0	2	0	0	0	0	0	outer membrane enzyme PagP beta-barrel family protein	0	2.33	0.87	0.76	0.78		236	0
SNOO_001310A	C	1	1	1	1	3	8	14	102	5	8	3	18	12	MoCDIP4-like glucanase	0	2.33	0.3	0.6	0.89		229	4
SNOO_149380A	C	1	1	1	1	3	8	14	102	5	8	3	18	12	MoCDIP4-like glucanase	0	2.33	0.4	0.67	0.89	C	220	4
SNOO_108620A	C	1	1	1	1	3	8	14	102	5	8	3	18	12	CfTom1-like xylanase	0	2.29	0.01	0.62	0.63		332	4
SNOO_152700A	C	1	1	1	1	3	8	14	102	5	8	3	18	12	FgXYLA-like xylanase	0	2.26	0.76	0.78	0.75		231	0
SNOO_010970A	C	1	1	1	1	3	8	14	102	5	8	3	18	12	Tox3-like protein	1	2.23	0.52	0.64	0.25	C	224	6
SNOO_086040A	A	1	1	1	1	3	8	14	102	5	8	3	17	12	FgXYLA-like xylanase	0	2.15	0.25	0.71	0.77		258	1
SNOO_019220A	C	1	1	1	1	3	8	14	102	5	8	3	18	12	MoCDIP4-like glucanase	0	2.1	0.21	0.56	0.8		258	2
SNOO_002000A	C	1	1	1	1	3	8	14	102	5	8	3	18	12	VdPevD1-like Alternaria alternata allergen 1 family protein	0	1.85	0.71	0.56	0.87		168	6
SNOO_575600	S	0	0	0	0	0	2	0	0	0	0	0	0	0	acetylxylan esterase	0	1.83	0.02	0.62	0.74		302	4
SNOO_160810A	C	1	1	1	1	3	8	14	102	5	8	3	18	12	MoCDIP4-like glucanase	0	1.83	0.06	0.58	0.78		238	5
SNOO_098820A	C	1	1	1	1	3	8	14	102	5	8	3	18	12	MoCDIP4-like pectin lyase	0	1.82	0.01	0.57	0.91	C	358	9
SNOO_008150A	C	1	1	1	1	3	8	14	102	5	8	3	18	12	MoCDIP4-like glucanase	0	1.77	0	0.24	0.83		234	2
SNOO_026870A	C	1	1	1	1	3	8	14	102	5	8	3	18	12	MoCDIP4-like glucanase	0	1.77	0.06	0.33	0.8		222	2
SNOO_423720A	A	1	1	1	1	3	8	14	102	5	8	3	16	12	LysM domain superfamily protein	1	1.75	0.95	0.67	0.58		113	5
SNOO_108650A	C	1	1	1	1	3	8	14	102	5	8	3	18	12	FgXYLA-like xylanase	0	1.68	0.04	0.56	0.76		231	2
SNOO_065020A	C	1	1	1	1	3	8	14	102	5	8	3	18	12	FGL1-like lipase	0	1.63	0	0.36	0.8		304	6
SNOO_503200	A	0	0	1	0	3	8	14	102	5	0	3	16	12	Tox3-like protein	0	1.63	1	0.71	0.21		161	4
SNOO_510220	A	0	0	0	0	0	8	14	33	5	0	3	7	0	acetylcholinesterase/carboxylesterase	1	1.63	0.81	0.67	0.23		199	5
SNOO_159340A	C	1	1	1	1	3	8	14	102	5	8	3	18	12	CfTom1-like xylanase	0	1.56	0.09	0.55	0.76		322	2
SNOO_140400A	C	1	1	1	1	3	8	14	102	5	8	3	18	12	FgXYLA-like xylanase	0	1.54	0	0.24	0.86		227	2
SNOO_100710A	C	1	1	1	1	3	8	14	102	5	8	3	18	12	MoCDIP4-like glucanase	0	1.5	0.07	0.45	0.87		249	4
SNOO_123500A	C	1	1	1	1	3	8	14	102	5	8	3	18	12	MoBas2-like protein	0	1.49	0.88	0.24	0.85		103	6
SNOO_035930A	C	1	1	1	1	3	8	14	102	5	8	3	18	12	CfTom1-like xylanase	0	1.31	0	0.5	0.75		355	4
SNOO_102410A	C	1	1	1	1	3	8	14	102	5	8	3	18	12	Zt6-like endoribonuclease	0	1.27	0.08	0.45	0.72		133	4
SNOO_098950A	C	1	1	1	1	3	8	14	102	5	8	3	18	12	NEP-like protein	0	1.25	0.02	0.37	0.76		233	2
SNOO_069800A	C	1	1	1	1	3	8	14	102	5	8	3	18	12	CfTom1-like xylanase	0	1.1	0	0.1	0.89		393	0
SNOO_550640	A	0	0	0	0	0	0	0	5	0	0	0	0	0	RWD-like superfamily protein	1	1.09	1	0.57	0.44		7	0
SNOO_059190A	C	1	1	1	1	3	8	14	102	5	8	3	18	12	MoCDIP4-like glucanase	0	1.05	0.2	0.53	0.48		254	4
SNOO_057170AB	S	1	0	0	0	0	0	0	0	0	1	0	0	0	PLAC8 motif-containing protein	0	1.04	1	0.91	0.38		91	9
SNOO_105220A	A	1	1	1	1	3	8	14	102	5	8	3	17	12	AVR-Pita2-like peptidase	0	1.03	0	0.16	0.85		350	8

[a](C)ore, (A)ccessory, or (S)ingleton pangenome based on whether an orthogroup was present in all, some, or one isolate.

[b]Multi-copy orthogroups have more than one member in at least one isolate.

[c]Presence or absence of the orthogroup in the four reference isolates.

[d]Numbers of isolates with an orthogroup copy in each of the population clusters. The reference isolates were not included in the STRUCTURE analysis, so SN15 was assigned to cluster 6 where it was assigned by Phan et al. (2020), and the remaining reference isolates were assigned to cluster 8 with the international isolates.

[e]tests for positive selection in orthogroups were significant ($p<0.01$, number members in orthogroup > 0.1)

[f]N=nuclear localized, C=chloroplast localized

Author Statements

Authors and Contributors

DABJ, JKH, K-CT, and HTTP conceived and designed the study. KR and HTTP performed laboratory work. DABJ, SB, and JKH performed bioinformatics and data analysis. DABJ and JKH wrote the manuscript. DABJ, K-CT, HTTP, and JKH edited the manuscript. All authors read and approved the manuscript.

Conflicts of Interest

The authors declare there are no conflicts of interest.

Funding Information

This study was supported by the Centre for Crop and Disease Management, a joint initiative of Curtin University and the Grains Research and Development Corporation (Research Grant CUR00023). This research was undertaken with the assistance of resources and services from the Pawsey Supercomputing Centre and the National Computational Infrastructure (NCI), which is supported by the Australian Government. This research is supported by an Australian Government Research Training Program (RTP) Scholarship.

Ethical Approval

n/a

Parsed Citations

Abeysekara, N. S., T. L. Friesen, B. Keller and J. D. Faris (2009). "Identification and characterization of a novel host–toxin interaction in the wheat–Stagonospora nodorum pathosystem." Theoretical and Applied Genetics 120(1): 117-126.
Google Scholar: Author Only Title Only Author and Title

Agapow, P.-M. and A. Burt (2001). "Indices of multilocus linkage disequilibrium." Molecular Ecology Notes 1(1-2): 101-102.
Google Scholar: Author Only Title Only Author and Title

Almagro Armenteros, J. J., C. K. Sønderby, S. K. Sønderby, H. Nielsen and O. Winther (2017). "DeepLoc: prediction of protein subcellular localization using deep learning." Bioinformatics 33(21): 3387-3395.
Google Scholar: Author Only Title Only Author and Title

Armenteros, J. J. A., M. Salvatore, O. Emanuelsson, O. Winther, G. Von Heijne, A. Elofsson and H. Nielsen (2019). "Detecting sequence signals in targeting peptides using deep learning." Life science alliance 2(5).

Armenteros, J. J. A., K. D. Tsirigos, C. K. Sønderby, T. N. Petersen, O. Winther, S. Brunak, G. von Heijne and H. Nielsen (2019). "SignalP 5.0 improves signal peptide predictions using deep neural networks." Nature biotechnology 37(4): 420-423.
Google Scholar: Author Only Title Only Author and Title

Aylward, J., E. T. Steenkamp, L. L. Dreyer, F. Roets, B. D. Wingfield and M. J. Wingfield (2017). "A plant pathology perspective of fungal genome sequencing." IMA Fungus 8(1): 1-15.
Google Scholar: Author Only Title Only Author and Title

Badet, T. and D. Croll (2020). "The rise and fall of genes: origins and functions of plant pathogen pangenomes." Current Opinion in Plant Biology 56: 65-73.
Google Scholar: Author Only Title Only Author and Title

Bairoch, A. and R. Apweiler (2000). "The SWISS-PROT protein sequence database and its supplement TrEMBL in 2000." Nucleic acids research 28(1): 45-48.
Google Scholar: Author Only Title Only Author and Title

Bankevich, A., S. Nurk, D. Antipov, A. A. Gurevich, M. Dvorkin, A. S. Kulikov, V. M. Lesin, S. I. Nikolenko, S. Pham, A. D. Prjibelski, A. V. Pyshkin, A. V. Sirotkin, N. Vyahhi, G. Tesler, M. A. Alekseyev and P. A. Pevzner (2012). "SPAdes: A New Genome Assembly Algorithm and Its Applications to Single-Cell Sequencing." Journal of Computational Biology 19(5): 455-477.
Google Scholar: Author Only Title Only Author and Title

Bathgate, J. A. and R. Loughman (2001). "Ascospores are a source of inoculum of Phaeosphaeria nodorum, P. avenaria f. sp. avenaria and Mycosphaerella graminicola in Western Australia." Australasian Plant Pathology 30(4): 317.
Google Scholar: Author Only Title Only Author and Title

Bennett, R. S., M. G. Milgroom and G. C. Bergstrom (2005). "Population Structure of Seedborne Phaeosphaeria nodorum on New York Wheat." Phytopathology 95(3): 300-305.
Google Scholar: Author Only Title Only Author and Title

Bertazzoni, S., D. A. Jones, H. T. Phan, K.-C. Tan and J. K. Hane (2021). "Chromosome-level genome assembly and manually-curated proteome of model necrotroph Parastagonospora nodorum Sn15 reveals a genome-wide trove of candidate effector homologs, and redundancy of virulence-related functions within an accessory chromosome." BMC genomics 22(1): 1-16.
Google Scholar: Author Only Title Only Author and Title

Bertazzoni, S., A. H. Williams, D. A. Jones, R. A. Syme, K.-C. Tan and J. K. Hane (2018). "Accessories make the outfit: accessory chromosomes and other dispensable DNA regions in plant-pathogenic Fungi." Molecular Plant-Microbe Interactions 31(8): 779-788.
Google Scholar: Author Only Title Only Author and Title

Bringans, S., J. K. Hane, T. Casey, K.-C. Tan, R. Lipscombe, P. S. Solomon and R. P. Oliver (2009). "Deep proteogenomics; high throughput gene validation by multidimensional liquid chromatography and mass spectrometry of proteins from the fungal wheat pathogen Stagonospora nodorum." BMC Bioinformatics 10(1): 301.
Google Scholar: Author Only Title Only Author and Title

Bu, B., D. Qiu, H. Zeng, L. Guo, J. Yuan and X. Yang (2014). "A fungal protein elicitor PevD1 induces Verticillium wilt resistance in cotton." Plant Cell Reports 33(3): 461-470.
Google Scholar: Author Only Title Only Author and Title

Buchfink, B., K. Reuter and H.-G. Drost (2021). "Sensitive protein alignments at tree-of-life scale using DIAMOND." Nature methods 18(4): 366-368.
Google Scholar: Author Only Title Only Author and Title

Bushnell, B., J. Rood and E. Singer (2017). "BBMerge – Accurate paired shotgun read merging via overlap." PLOS ONE 12(10): e0185056.
Google Scholar: Author Only Title Only Author and Title

Camacho, C., G. Coulouris, V. Avagyan, N. Ma, J. Papadopoulos, K. Bealer and T. L. Madden (2009). "BLAST+: architecture and applications." BMC Bioinformatics 10(1): 421.

Google Scholar: Author Only Title Only Author and Title

Caten, C. and A. Newton (2000). "Variation in cultural characteristics, pathogenicity, vegetative compatibility and electrophoretic karyotype within field populations of Stagonospora nodorum." Plant Pathology 49(2): 219-226.
Google Scholar: Author Only Title Only Author and Title

Chen, C., B. Lian, J. Hu, H. Zhai, X. Wang, R. C. Venu, E. Liu, Z. Wang, M. Chen, B. Wang, G.-L. Wang, Z. Wang and T. K. Mitchell (2013). "Genome comparison of two Magnaporthe oryzae field isolates reveals genome variations and potential virulence effectors." BMC Genomics 14(1): 887.
Google Scholar: Author Only Title Only Author and Title

Chen, S., P. Songkumarn, R. C. Venu, M. Gowda, M. Bellizzi, J. Hu, W. Liu, D. Ebbole, B. Meyers, T. Mitchell and G.-L. Wang (2013). "Identification and Characterization of In planta–Expressed Secreted Effector Proteins from Magnaporthe oryzae That Induce Cell Death in Rice." Molecular Plant-Microbe Interactions 26(2): 191-202.
Google Scholar: Author Only Title Only Author and Title

Chooi, Y.-H., M. J. Muria-Gonzalez and P. S. Solomon (2014). "A genome-wide survey of the secondary metabolite biosynthesis genes in the wheat pathogen Parastagonospora nodorum." Mycology 5(3): 192-206.
Google Scholar: Author Only Title Only Author and Title

Chuma, I., C. Isobe, Y. Hotta, K. Ibaragi, N. Futamata, M. Kusaba, K. Yoshida, R. Terauchi, Y. Fujita, H. Nakayashiki, B. Valent and Y. Tosa (2011). "Multiple Translocation of the AVR-Pita Effector Gene among Chromosomes of the Rice Blast Fungus Magnaporthe oryzae and Related Species." PLOS Pathogens 7(7): e1002147.
Google Scholar: Author Only Title Only Author and Title

Cingolani, P., A. Platts, L. L. Wang, M. Coon, T. Nguyen, L. Wang, S. J. Land, X. Lu and D. M. Ruden (2012). "A program for annotating and predicting the effects of single nucleotide polymorphisms, SnpEff." Fly 6(2): 80-92.
Google Scholar: Author Only Title Only Author and Title

Croll, D., M. Zala and B. A. McDonald (2013). "Breakage-fusion-bridge cycles and large insertions contribute to the rapid evolution of accessory chromosomes in a fungal pathogen." PLoS Genetics 9(6): e1003567.
Google Scholar: Author Only Title Only Author and Title

Cunfer, B. M. (1978). "The Incidence of Septoria nodorum in Wheat Seed." Phytopathology 68(6): 832.
Google Scholar: Author Only Title Only Author and Title

Cunfer, B. M. (1998). "Seasonal availability of inoculum of Stagonospora nodorum in the field in the southeastern US." Cereal Research Communications 26(3): 259-263.
Google Scholar: Author Only Title Only Author and Title

Dai, Y., Y. Jia, J. Correll, X. Wang and Y. Wang (2010). "Diversification and evolution of the avirulence gene AVR-Pita1 in field isolates of Magnaporthe oryzae." Fungal Genetics and Biology 47(12): 973-980.
Google Scholar: Author Only Title Only Author and Title

Dalman, K., K. Himmelstrand, Å. Olson, M. Lind, M. Brandström-Durling and J. Stenlid (2013). "A Genome-Wide Association Study Identifies Genomic Regions for Virulence in the Non-Model Organism Heterobasidion annosum s.s." PLOS ONE 8(1): e53525.
Google Scholar: Author Only Title Only Author and Title

de Guillen, K., D. Ortiz-Vallejo, J. Gracy, E. Fournier, T. Kroj and A. Padilla (2015). "Structure analysis uncovers a highly diverse but structurally conserved effector family in phytopathogenic fungi." PLoS pathogens 11(10): e1005228.
Google Scholar: Author Only Title Only Author and Title

Dierckxsens, N., P. Mardulyn and G. Smits (2017). "NOVOPlasty: de novo assembly of organelle genomes from whole genome data." Nucleic Acids Research 45(4): e18-e18.
Google Scholar: Author Only Title Only Author and Title

Dobin, A., C. A. Davis, F. Schlesinger, J. Drenkow, C. Zaleski, S. Jha, P. Batut, M. Chaisson and T. R. Gingeras (2013). "STAR: ultrafast universal RNA-seq aligner." Bioinformatics 29(1): 15-21.
Google Scholar: Author Only Title Only Author and Title

Earl, D. A. and B. M. vonHoldt (2012). "STRUCTURE HARVESTER: a website and program for visualizing STRUCTURE output and implementing the Evanno method." Conservation Genetics Resources 4(2): 359-361.
Google Scholar: Author Only Title Only Author and Title

Eberhardt, R. Y., D. H. Haft, M. Punta, M. Martin, C. O'Donovan and A. Bateman (2012). "AntiFam: a tool to help identify spurious ORFs in protein annotation." Database 2012.
Google Scholar: Author Only Title Only Author and Title

Ellinghaus, D., S. Kurtz and U. Willhoeft (2008). "LTRharvest, an efficient and flexible software for de novo detection of LTR retrotransposons." BMC Bioinformatics 9(1): 18.
Google Scholar: Author Only Title Only Author and Title

Evanno, G., S. Regnaut and J. Goudet (2005). "Detecting the number of clusters of individuals using the software structure: a simulation study." Molecular Ecology 14(8): 2611-2620.

Google Scholar: Author Only Title Only Author and Title

Ewels, P., M. Magnusson, S. Lundin and M. Käller (2016). "MultiQC: summarize analysis results for multiple tools and samples in a single report." Bioinformatics 32(19): 3047-3048.
Google Scholar: Author Only Title Only Author and Title

Fenton, A., J. Antonovics and Michael A. Brockhurst (2009). "Inverse-Gene-for-Gene Infection Genetics and Coevolutionary Dynamics." The American Naturalist 174(6): E230-E242.
Google Scholar: Author Only Title Only Author and Title

Friesen, T. L., C. Chu, S. S. Xu and J. D. Faris (2012). "SnTox5–Snn5: a novel S tagonospora nodorum effector–wheat gene interaction and its relationship with the SnToxA–Tsn1 and SnTox3–Snn3–B1 interactions." Molecular Plant Pathology 13(9): 1101-1109.
Google Scholar: Author Only Title Only Author and Title

Friesen, T. L., S. W. Meinhardt and J. D. Faris (2007). "The Stagonospora nodorum-wheat pathosystem involves multiple proteinaceous host-selective toxins and corresponding host sensitivity genes that interact in an inverse gene-for-gene manner." The Plant Journal 51(4): 681-692.
Google Scholar: Author Only Title Only Author and Title

Friesen, T. L., Z. Zhang, P. S. Solomon, R. P. Oliver and J. D. Faris (2008). "Characterization of the interaction of a novel Stagonospora nodorum host-selective toxin with a wheat susceptibility gene." Plant physiology 146(2): 682-693.
Google Scholar: Author Only Title Only Author and Title

Galili, T. (2015). "dendextend: an R package for visualizing, adjusting and comparing trees of hierarchical clustering." Bioinformatics 31(22): 3718-3720.
Google Scholar: Author Only Title Only Author and Title

Gao, Y., J. Faris, Z. Liu, Y. Kim, R. Syme, R. Oliver, S. Xu and T. Friesen (2015). "Identification and characterization of the SnTox6-Snn6 interaction in the Parastagonospora nodorum–wheat pathosystem." Molecular Plant-Microbe Interactions 28(5): 615-625.
Google Scholar: Author Only Title Only Author and Title

Gervais, J., C. Plissonneau, J. Linglin, M. Meyer, K. Labadie, C. Cruaud, I. Fudal, T. Rouxel and M. H. Balesdent (2017). "Different waves of effector genes with contrasted genomic location are expressed by Leptosphaeria maculans during cotyledon and stem colonization of oilseed rape." Molecular plant pathology 18(8): 1113-1126.
Google Scholar: Author Only Title Only Author and Title

Ghaderi, F., B. Sharifnabi, M. Javan-Nikkhah, P. C. Brunner and B. A. McDonald (2020). "SnToxA ,SnTox1, and SnTox3 originated in Parastagonospora nodorum in the Fertile Crescent." Plant Pathology: ppa.13233.
Google Scholar: Author Only Title Only Author and Title

Grabherr, M. G., B. J. Haas, M. Yassour, J. Z. Levin, D. A. Thompson, I. Amit, X. Adiconis, L. Fan, R. Raychowdhury, Q. Zeng, Z. Chen, E. Mauceli, N. Hacohen, A. Gnirke, N. Rhind, F. d. Palma, B. W. Birren, C. Nusbaum, K. Lindblad-Toh, N. Friedman and A. Regev (2011). "Full-length transcriptome assembly from RNA-Seq data without a reference genome." Nature Biotechnology 29(7): 644-652.
Google Scholar: Author Only Title Only Author and Title

Gremme, G., S. Steinbiss and S. Kurtz (2013). "GenomeTools: A Comprehensive Software Library for Efficient Processing of Structured Genome Annotations." IEEE/ACM Transactions on Computational Biology and Bioinformatics 10(3): 645-656.
Google Scholar: Author Only Title Only Author and Title

Gu, Z., L. Gu, R. Eils, M. Schlesner and B. Brors (2014). "circlize implements and enhances circular visualization in R." Bioinformatics 30(19): 2811-2812.
Google Scholar: Author Only Title Only Author and Title

Gummer, J. P. A., R. D. Trengove, R. P. Oliver and P. S. Solomon (2013). "Dissecting the role of G-protein signalling in primary metabolism in the wheat pathogen Stagonospora nodorum." Microbiology 159(Pt_9): 1972-1985.
Google Scholar: Author Only Title Only Author and Title

Gurevich, A., V. Saveliev, N. Vyahhi and G. Tesler (2013). "QUAST: quality assessment tool for genome assemblies." Bioinformatics 29(8): 1072-1075.
Google Scholar: Author Only Title Only Author and Title

Guy St C, S. and B. Ewan (2005). "Automated generation of heuristics for biological sequence comparison." BMC Bioinformatics 6: 31-31.
Google Scholar: Author Only Title Only Author and Title

Haas, B. J., A. L. Delcher, S. M. Mount, J. R. Wortman, R. K. Smith Jr, L. I. Hannick, R. Maiti, C. M. Ronning, D. B. Rusch, C. D. Town, S. L. Salzberg and O. White (2003). "Improving the Arabidopsis genome annotation using maximal transcript alignment assemblies." Nucleic Acids Research 31(19): 5654-5666.
Google Scholar: Author Only Title Only Author and Title

Haas, B. J., S. L. Salzberg, W. Zhu, M. Pertea, J. E. Allen, J. Orvis, O. White, C. R. Buell and J. R. Wortman (2008). "Automated eukaryotic gene structure annotation using EVidenceModeler and the Program to Assemble Spliced Alignments." Genome Biology 9(1): R7.
Google Scholar: Author Only Title Only Author and Title

Hane, J. K., R. G. T. Lowe, P. S. Solomon, K.-C. Tan, C. L. Schoch, J. W. Spatafora, P. W. Crous, C. Kodira, B. W. Birren, J. E. Galagan, S. F. F. Torriani, B. A. McDonald and R. P. Oliver (2007). "Dothideomycete–Plant Interactions Illuminated by Genome Sequencing and EST Analysis of the Wheat Pathogen Stagonospora nodorum." The Plant Cell 19(11): 3347-3368.
Google Scholar: Author Only Title Only Author and Title

Hane, J. K., T. Rouxel, B. J. Howlett, G. H. Kema, S. B. Goodwin and R. P. Oliver (2011). "A novel mode of chromosomal evolution peculiar to filamentous Ascomycete fungi." Genome biology 12(5): 1-16.
Google Scholar: Author Only Title Only Author and Title

Hane, J. K., A. H. Williams, A. P. Taranto, P. S. Solomon and R. P. Oliver (2015). Repeat-induced point mutation: a fungal-specific, endogenous mutagenesis process. Genetic Transformation Systems in Fungi, Volume 2, Springer: 55-68.
Google Scholar: Author Only Title Only Author and Title

Hedrick, P. W. (2005). "A standardized genetic differentiation measure." Evolution 59(8): 1633-1638.
Google Scholar: Author Only Title Only Author and Title

Hoang, D. T., O. Chernomor, A. Von Haeseler, B. Q. Minh and L. S. Vinh (2018). "UFBoot2: improving the ultrafast bootstrap approximation." Molecular biology and evolution 35(2): 518-522.
Google Scholar: Author Only Title Only Author and Title

Hocher, A. and A. Taddei (2020). "Subtelomeres as specialized chromatin domains." BioEssays 42(5): 1900205.
Google Scholar: Author Only Title Only Author and Title

Hu, J., Y. Zheng and X. Shang (2018). "MiteFinderII: a novel tool to identify miniature inverted-repeat transposable elements hidden in eukaryotic genomes." BMC Medical Genomics 11(5): 101.
Google Scholar: Author Only Title Only Author and Title

Huerta-Cepas, J., K. Forslund, L. P. Coelho, D. Szklarczyk, L. J. Jensen, C. Von Mering and P. Bork (2017). "Fast genome-wide functional annotation through orthology assignment by eggNOG-mapper." Molecular biology and evolution 34(8): 2115-2122.
Google Scholar: Author Only Title Only Author and Title

Hurlbert, S. H. (1971). "The Nonconcept of Species Diversity: A Critique and Alternative Parameters." Ecology 52(4): 577-586.
Google Scholar: Author Only Title Only Author and Title

Ipcho, S. V. S., J. K. Hane, E. A. Antoni, D. Ahren, B. Henrissat, T. L. Friesen, P. S. Solomon and R. P. Oliver (2012). "Transcriptome analysis of Stagonospora nodorum: gene models, effectors, metabolism and pantothenate dispensability." Molecular Plant Pathology 13(6): 531-545.
Google Scholar: Author Only Title Only Author and Title

Irieda, H., Y. Inoue, M. Mori, K. Yamada, Y. Oshikawa, H. Saitoh, A. Uemura, R. Terauchi, S. Kitakura, A. Kosaka, S. Singkaravanit-Ogawa and Y. Takano (2019). "Conserved fungal effector suppresses PAMP-triggered immunity by targeting plant immune kinases." Proceedings of the National Academy of Sciences 116(2): 496-505.
Google Scholar: Author Only Title Only Author and Title

Iwata, H. and O. Gotoh (2012). "Benchmarking spliced alignment programs including Spaln2, an extended version of Spaln that incorporates additional species-specific features." Nucleic Acids Research 40(20): e161-e161.
Google Scholar: Author Only Title Only Author and Title

Jain, C., S. Koren, A. Dilthey, A. M. Phillippy and S. Aluru (2018). "A fast adaptive algorithm for computing whole-genome homology maps." Bioinformatics 34(17): i748-i756.
Google Scholar: Author Only Title Only Author and Title

Jombart, T. (2008). "adegenet: a R package for the multivariate analysis of genetic markers." Bioinformatics 24(11): 1403-1405.
Google Scholar: Author Only Title Only Author and Title

Jones, D. A. B., S. Bertazzoni, C. J. Turo, R. A. Syme and J. K. Hane (2018). "Bioinformatic prediction of plant–pathogenicity effector proteins of fungi." Current Opinion in Microbiology 46: 43-49.
Google Scholar: Author Only Title Only Author and Title

Jones, D. A. B., E. John, K. Rybak, H. T. T. Phan, K. B. Singh, S.-Y. Lin, P. S. Solomon, R. P. Oliver and K.-C. Tan (2019). "A specific fungal transcription factor controls effector gene expression and orchestrates the establishment of the necrotrophic pathogen lifestyle on wheat." Scientific Reports 9(1): 1-13.
Google Scholar: Author Only Title Only Author and Title

Jones, P., D. Binns, H.-Y. Chang, M. Fraser, W. Li, C. McAnulla, H. McWilliam, J. Maslen, A. Mitchell and G. Nuka (2014). "InterProScan 5: genome-scale protein function classification." Bioinformatics 30(9): 1236-1240.
Google Scholar: Author Only Title Only Author and Title

Käll, L., A. Krogh and E. L. Sonnhammer (2004). "A combined transmembrane topology and signal peptide prediction method." Journal of molecular biology 338(5): 1027-1036.
Google Scholar: Author Only Title Only Author and Title

Kalyaanamoorthy, S., B. Q. Minh, T. K. F. Wong, A. von Haeseler and L. S. Jermiin (2017). "ModelFinder: fast model selection for

accurate phylogenetic estimates." Nature Methods 14(6): 587-589.
Google Scholar: Author Only Title Only Author and Title

Kamvar, Z. N., J. F. Tabima and N. J. Grünwald (2014). "Poppr: an R package for genetic analysis of populations with clonal, partially clonal, and/or sexual reproduction." PeerJ 2: e281.
Google Scholar: Author Only Title Only Author and Title

Kanja, C. and K. E. Hammond-Kosack (2020). "Proteinaceous effector discovery and characterization in filamentous plant pathogens." Molecular Plant Pathology 21(10): 1353-1376.
Google Scholar: Author Only Title Only Author and Title

Keilwagen, J., F. Hartung, M. Paulini, S. O. Twardziok and J. Grau (2018). "Combining RNA-seq data and homology-based gene prediction for plants, animals and fungi." BMC Bioinformatics 19(1): 189.
Google Scholar: Author Only Title Only Author and Title

Keller, S. M., J. M. McDermott, R. Pettway, M. Wolfe and B. McDonald (1997). "Gene flow and sexual reproduction in the wheat glume blotch pathogen Phaeosphaeria nodorum (anamorph Stagonospora nodorum)." Phytopathology 87(3): 353-358.
Google Scholar: Author Only Title Only Author and Title

Kettles, G. J., C. Bayon, C. A. Sparks, G. Canning, K. Kanyuka and J. J. Rudd (2018). "Characterization of an antimicrobial and phytotoxic ribonuclease secreted by the fungal wheat pathogen Zymoseptoria tritici." New Phytologist 217(1): 320-331.
Google Scholar: Author Only Title Only Author and Title

Kim, S., H. Park, H. A. Gruszewski, D. G. Schmale and S. Jung (2019). "Vortex-induced dispersal of a plant pathogen by raindrop impact." Proceedings of the National Academy of Sciences 116(11): 4917-4922.
Google Scholar: Author Only Title Only Author and Title

Klopfenstein, D. V., L. Zhang, B. S. Pedersen, F. Ramírez, A. Warwick Vesztrocy, A. Naldi, C. J. Mungall, J. M. Yunes, O. Botvinnik, M. Weigel, W. Dampier, C. Dessimoz, P. Flick and H. Tang (2018). "GOATOOLS: A Python library for Gene Ontology analyses." Scientific Reports 8(1): 10872.
Google Scholar: Author Only Title Only Author and Title

Knaus, B. J. and N. J. Grünwald (2017). "vcfr: a package to manipulate and visualize variant call format data in R." Molecular Ecology Resources 17(1): 44-53.
Google Scholar: Author Only Title Only Author and Title

Koskinen, P., P. Törönen, J. Nokso-Koivisto and L. Holm (2015). "PANNZER: high-throughput functional annotation of uncharacterized proteins in an error-prone environment." Bioinformatics 31(10): 1544-1552.
Google Scholar: Author Only Title Only Author and Title

Krogh, A., B. Larsson, G. Von Heijne and E. L. Sonnhammer (2001). "Predicting transmembrane protein topology with a hidden Markov model: application to complete genomes." Journal of molecular biology 305(3): 567-580.
Google Scholar: Author Only Title Only Author and Title

Lagesen, K., P. Hallin, E. A. Rødland, H.-H. Stærfeldt, T. Rognes and D. W. Ussery (2007). "RNAmmer: consistent and rapid annotation of ribosomal RNA genes." Nucleic Acids Research 35(9): 3100-3108.
Google Scholar: Author Only Title Only Author and Title

Lechner, M., S. Findeiß, L. Steiner, M. Marz, P. F. Stadler and S. J. Prohaska (2011). "Proteinortho: detection of (co-) orthologs in large-scale analysis." BMC bioinformatics 12(1): 1-9.
Google Scholar: Author Only Title Only Author and Title

Li, H. (2011). "A statistical framework for SNP calling, mutation discovery, association mapping and population genetical parameter estimation from sequencing data." Bioinformatics 27(21): 2987-2993.
Google Scholar: Author Only Title Only Author and Title

Li, H. (2018). "Minimap2: pairwise alignment for nucleotide sequences." Bioinformatics 34(18): 3094-3100.
Google Scholar: Author Only Title Only Author and Title

Li, H., B. Handsaker, A. Wysoker, T. Fennell, J. Ruan, N. Homer, G. Marth, G. Abecasis and R. Durbin (2009). "The Sequence Alignment/Map format and SAMtools." Bioinformatics 25(16): 2078-2079.
Google Scholar: Author Only Title Only Author and Title

Liu, Z., J. D. Faris, R. P. Oliver, K.-C. Tan, P. S. Solomon, M. C. McDonald, B. A. McDonald, A. Nunez, S. Lu and J. B. Rasmussen (2009). "SnTox3 acts in effector triggered susceptibility to induce disease on wheat carrying the Snn3 gene." PLoS pathogens 5(9): e1000581.
Google Scholar: Author Only Title Only Author and Title

Liu, Z., T. L. Friesen, H. Ling, S. W. Meinhardt, R. P. Oliver, J. B. Rasmussen and J. D. Faris (2006). "The Tsn1–ToxA interaction in the wheat–Stagonospora nodorum pathosystem parallels that of the wheat–tan spot system." Genome 49(10): 1265-1273.
Google Scholar: Author Only Title Only Author and Title

Liu, Z., Z. Zhang, J. D. Faris, R. P. Oliver, R. Syme, M. C. McDonald, B. A. McDonald, P. S. Solomon, S. Lu and W. L. Shelver (2012). "The cysteine rich necrotrophic effector SnTox1 produced by Stagonospora nodorum triggers susceptibility of wheat lines harboring Snn1." PLoS pathogens 8(1): e1002467.

Google Scholar: Author Only Title Only Author and Title

Llorens, C., R. Futami, L. Covelli, L. Domínguez-Escribá, J. M. Viu, D. Tamarit, J. Aguilar-Rodríguez, M. Vicente-Ripolles, G. Fuster, G. P. Bernet, F. Maumus, A. Munoz-Pomer, J. M. Sempere, A. Latorre and A. Moya (2011). "The Gypsy Database (GyDB) of mobile genetic elements: release 2.0." Nucleic Acids Research 39(suppl_1): D70-D74.

Lomsadze, A., P. D. Burns and M. Borodovsky (2014). "Integration of mapped RNA-Seq reads into automatic training of eukaryotic gene finding algorithm." Nucleic Acids Research 42(15): e119-e119.
Google Scholar: Author Only Title Only Author and Title

Lowe, R. G. T., M. Lord, K. Rybak, R. D. Trengove, R. P. Oliver and P. S. Solomon (2008). "A metabolomic approach to dissecting osmotic stress in the wheat pathogen Stagonospora nodorum." Fungal Genetics and Biology 45(11): 1479-1486.
Google Scholar: Author Only Title Only Author and Title

Lowe, T. M. and P. P. Chan (2016). "tRNAscan-SE On-line: integrating search and context for analysis of transfer RNA genes." Nucleic Acids Research 44(W1): W54-W57.

Lunter, G. and M. Goodson (2011). "Stampy: A statistical algorithm for sensitive and fast mapping of Illumina sequence reads." Genome Research 21(6): 936-939.
Google Scholar: Author Only Title Only Author and Title

M'Barek, S. B., J. H. Cordewener, S. M. T. Ghaffary, T. A. van der Lee, Z. Liu, A. M. Gohari, R. Mehrabi, A. H. America, O. Robert and T. L. Friesen (2015). "FPLC and liquid-chromatography mass spectrometry identify candidate necrosis-inducing proteins from culture filtrates of the fungal wheat pathogen Zymoseptoria tritici." Fungal Genetics and Biology 79: 54-62.
Google Scholar: Author Only Title Only Author and Title

Mapleson, D., G. Garcia Accinelli, G. Kettleborough, J. Wright and B. J. Clavijo (2017). "KAT: a K-mer analysis toolkit to quality control NGS datasets and genome assemblies." Bioinformatics 33(4): 574-576.
Google Scholar: Author Only Title Only Author and Title

Marçais, G., A. L. Delcher, A. M. Phillippy, R. Coston, S. L. Salzberg and A. Zimin (2018). "MUMmer4: A fast and versatile genome alignment system." PLOS Computational Biology 14(1): e1005944.
Google Scholar: Author Only Title Only Author and Title

Martin, M. (2011). "Cutadapt removes adapter sequences from high-throughput sequencing reads." EMBnet.journal 17(1): 10-12.
Google Scholar: Author Only Title Only Author and Title

McClintock, B. (1941). "The stability of broken ends of chromosomes in Zea mays." Genetics 26(2): 234.
Google Scholar: Author Only Title Only Author and Title

McDonald, M. C., M. Razavi, T. L. Friesen, P. C. Brunner and B. A. McDonald (2012). "Phylogenetic and population genetic analyses of Phaeosphaeria nodorum and its close relatives indicate cryptic species and an origin in the Fertile Crescent." Fungal Genet Biol 49(11): 882-895.
Google Scholar: Author Only Title Only Author and Title

McKenna, A., M. Hanna, E. Banks, A. Sivachenko, K. Cibulskis, A. Kernytsky, K. Garimella, D. Altshuler, S. Gabriel, M. Daly and M. A. DePristo (2010). "The Genome Analysis Toolkit: A MapReduce framework for analyzing next-generation DNA sequencing data." Genome Research 20(9): 1297-1303.
Google Scholar: Author Only Title Only Author and Title

Minh, B. Q., H. A. Schmidt, O. Chernomor, D. Schrempf, M. D. Woodhams, A. von Haeseler and R. Lanfear (2020). "IQ-TREE 2: New Models and Efficient Methods for Phylogenetic Inference in the Genomic Era." Molecular Biology and Evolution 37(5): 1530-1534.
Google Scholar: Author Only Title Only Author and Title

Mistry, J., R. D. Finn, S. R. Eddy, A. Bateman and M. Punta (2013). "Challenges in homology search: HMMER3 and convergent evolution of coiled-coil regions." Nucleic acids research 41(12): e121-e121.
Google Scholar: Author Only Title Only Author and Title

Mitchell, A. L., T. K. Attwood, P. C. Babbitt, M. Blum, P. Bork, A. Bridge, S. D. Brown, H.-Y. Chang, S. El-Gebali and M. I. Fraser (2019). "InterPro in 2019: improving coverage, classification and access to protein sequence annotations." Nucleic acids research 47(D1): D351-D360.
Google Scholar: Author Only Title Only Author and Title

Mosquera, G., M. C. Giraldo, C. H. Khang, S. Coughlan and B. Valent (2009). "Interaction transcriptome analysis identifies Magnaporthe oryzae BAS1-4 as biotrophy-associated secreted proteins in rice blast disease." The Plant Cell 21(4): 1273-1290.
Google Scholar: Author Only Title Only Author and Title

Muria-Gonzalez, M. J., Y. Yeng, S. Breen, O. Mead, C. Wang, Y.-H. Chooi, R. A. Barrow and P. S. Solomon (2020). "Volatile Molecules Secreted by the Wheat Pathogen Parastagonospora nodorum Are Involved in Development and Phytotoxicity." Frontiers in Microbiology 11.

Murphy, N., R. Loughman, R. Appels, E. Lagudah and M. Jones (2000). "Genetic variability in a collection of Stagonospora nodorum isolates from Western Australia." Australian journal of agricultural research 51(6): 679-684.

Google Scholar: Author Only Title Only Author and Title

Murray, G. M. and J. P. Brennan (2009). "Estimating disease losses to the Australian wheat industry." Australasian Plant Pathology 38(6): 558-570.
Google Scholar: Author Only Title Only Author and Title

Murrell, B., S. Moola, A. Mabona, T. Weighill, D. Sheward, S. L. Kosakovsky Pond and K. Scheffler (2013). "FUBAR: A Fast, Unconstrained Bayesian AppRoximation for Inferring Selection." Molecular Biology and Evolution 30(5): 1196-1205.
Google Scholar: Author Only Title Only Author and Title

Murrell, B., S. Weaver, M. D. Smith, J. O. Wertheim, S. Murrell, A. Aylward, K. Eren, T. Pollner, D. P. Martin, D. M. Smith, K. Scheffler and S. L. Kosakovsky Pond (2015). "Gene-Wide Identification of Episodic Selection." Molecular Biology and Evolution 32(5): 1365-1371.
Google Scholar: Author Only Title Only Author and Title

Ohm, R. A., N. Feau, B. Henrissat, C. L. Schoch, B. A. Horwitz, K. W. Barry, B. J. Condon, A. C. Copeland, B. Dhillon, F. Glaser, C. N. Hesse, I. Kosti, K. LaButti, E. A. Lindquist, S. Lucas, A. A. Salamov, R. E. Bradshaw, L. Ciuffetti, R. C. Hamelin, G. H. J. Kema, C. Lawrence, J. A. Scott, J. W. Spatafora, B. G. Turgeon, P. J. G. M. d. Wit, S. Zhong, S. B. Goodwin and I. V. Grigoriev (2012). "Diverse Lifestyles and Strategies of Plant Pathogenesis Encoded in the Genomes of Eighteen Dothideomycetes Fungi." PLOS Pathogens 8(12): e1003037.
Google Scholar: Author Only Title Only Author and Title

Ökmen, B., D. W. Etalo, M. H. A. J. Joosten, H. J. Bouwmeester, R. C. H. d. Vos, J. Collemare and P. J. G. M. d. Wit (2013). "Detoxification of α-tomatine by Cladosporium fulvum is required for full virulence on tomato." New Phytologist 198(4): 1203-1214.
Google Scholar: Author Only Title Only Author and Title

Oome, S., T. M. Raaymakers, A. Cabral, S. Samwel, H. Böhm, I. Albert, T. Nürnberger and G. Van den Ackerveken (2014). "Nep1-like proteins from three kingdoms of life act as a microbe-associated molecular pattern in Arabidopsis." Proceedings of the National Academy of Sciences of the United States of America 111(47): 16955-16960.
Google Scholar: Author Only Title Only Author and Title

Ou, S. and N. Jiang (2018). "LTR_retriever: A Highly Accurate and Sensitive Program for Identification of Long Terminal Repeat Retrotransposons." Plant Physiology 176(2): 1410-1422.
Google Scholar: Author Only Title Only Author and Title

Pareja-Jaime, Y., M. I. G. Roncero and M. C. Ruiz-Roldán (2008). "Tomatinase from Fusarium oxysporum f. sp. lycopersici is required for full virulence on tomato plants." Molecular plant-microbe interactions 21(6): 728-736.
Google Scholar: Author Only Title Only Author and Title

Pereira, D., B. A. McDonald and D. Croll (2020). "The genetic architecture of emerging fungicide resistance in populations of a global wheat pathogen." bioRxiv: 2020.2003.2026.010199.
Google Scholar: Author Only Title Only Author and Title

Pertea, M., G. M. Pertea, C. M. Antonescu, T.-c. Chang, J. T. Mendell and S. L. Salzberg (2015). "StringTie enables improved reconstruction of a transcriptome from RNA-seq reads." Nature Biotechnology 33(3): 290-295.
Google Scholar: Author Only Title Only Author and Title

Phan, H. T., K. Rybak, S. Bertazzoni, E. Furuki, E. Dinglasan, L. T. Hickey, R. P. Oliver and K.-C. Tan (2018). "Novel sources of resistance to Septoria nodorum blotch in the Vavilov wheat collection identified by genome-wide association studies." Theoretical and Applied Genetics 131(6): 1223-1238.
Google Scholar: Author Only Title Only Author and Title

Phan, H. T., K. Rybak, E. Furuki, S. Breen, P. S. Solomon, R. P. Oliver and K. C. Tan (2016). "Differential effector gene expression underpins epistasis in a plant fungal disease." The Plant Journal 87(4): 343-354.
Google Scholar: Author Only Title Only Author and Title

Phan, H. T. T., D. A. B. Jones, K. Rybak, K. N. Dodhia, F. J. Lopez-Ruiz, R. Valade, L. Gout, M.-H. Lebrun, P. C. Brunner, R. P. Oliver and K.-C. Tan (2020). "Low Amplitude Boom-and-Bust Cycles Define the Septoria Nodorum Blotch Interaction." Frontiers in Plant Science 10.

Pollet, A., T. Beliën, K. Fierens, J. A. Delcour and C. M. Courtin (2009). "Fusarium graminearum xylanases show different functional stabilities, substrate specificities and inhibition sensitivities." Enzyme and Microbial Technology 44(4): 189-195.
Google Scholar: Author Only Title Only Author and Title

Pond, S. L. K., S. D. W. Frost and S. V. Muse (2005). "HyPhy: hypothesis testing using phylogenies." Bioinformatics 21(5): 676-679.
Google Scholar: Author Only Title Only Author and Title

Poplin, R., V. Ruano-Rubio, M. A. DePristo, T. J. Fennell, M. O. Carneiro, G. A. V. d. Auwera, D. E. Kling, L. D. Gauthier, A. Levy-Moonshine, D. Roazen, K. Shakir, J. Thibault, S. Chandran, C. Whelan, M. Lek, S. Gabriel, M. J. Daly, B. Neale, D. G. MacArthur and E. Banks (2018). "Scaling accurate genetic variant discovery to tens of thousands of samples." bioRxiv: 201178.
Google Scholar: Author Only Title Only Author and Title

Praz, C. R., S. Bourras, F. Zeng, J. Sánchez-Martín, F. Menardo, M. Xue, L. Yang, S. Roffler, R. Böni and G. Herren (2017). "AvrPm2 encodes an RN ase-like avirulence effector which is conserved in the two different specialized forms of wheat and rye powdery

mildew fungus." New Phytologist 213(3): 1301-1314.
Google Scholar: Author Only Title Only Author and Title

Price, M. N., P. S. Dehal and A. P. Arkin (2010). "FastTree 2 – Approximately Maximum-Likelihood Trees for Large Alignments." PLOS ONE 5(3): e9490.
Google Scholar: Author Only Title Only Author and Title

Pritchard, J. K., M. Stephens and P. Donnelly (2000). "Inference of Population Structure Using Multilocus Genotype Data." Genetics 155(2): 945-959.
Google Scholar: Author Only Title Only Author and Title

Purcell, S., B. Neale, K. Todd-Brown, L. Thomas, M. A. R. Ferreira, D. Bender, J. Maller, P. Sklar, P. I. W. de Bakker, M. J. Daly and P. C. Sham (2007). "PLINK: A Tool Set for Whole-Genome Association and Population-Based Linkage Analyses." The American Journal of Human Genetics 81(3): 559-575.
Google Scholar: Author Only Title Only Author and Title

Quinlan, A. R. and I. M. Hall (2010). "BEDTools: a flexible suite of utilities for comparing genomic features." Bioinformatics 26(6): 841-842.
Google Scholar: Author Only Title Only Author and Title

Richards, J. K., E. H. Stukenbrock, J. Carpenter, Z. Liu, C. Cowger, J. D. Faris and T. L. Friesen (2019). "Local adaptation drives the diversification of effectors in the fungal wheat pathogen Parastagonospora nodorum in the United States." PLOS Genetics 15(10): e1008223.
Google Scholar: Author Only Title Only Author and Title

Richards, J. K., N. A. Wyatt, Z. Liu, J. D. Faris and T. L. Friesen (2018). "Reference Quality Genome Assemblies of Three Parastagonospora nodorum Isolates Differing in Virulence on Wheat." G3: Genes, Genomes, Genetics 8(2): 393-399.
Google Scholar: Author Only Title Only Author and Title

Rognes, T., T. Flouri, B. Nichols, C. Quince and F. Mahé (2016). "VSEARCH: a versatile open source tool for metagenomics." PeerJ 4: e2584.
Google Scholar: Author Only Title Only Author and Title

Sanger, F., A. R. Coulson, T. Friedmann, G. M. Air, B. G. Barrell, N. L. Brown, J. C. Fiddes, C. A. Hutchison, P. M. Slocombe and M. Smith (1978). "The nucleotide sequence of bacteriophage φX174." Journal of Molecular Biology 125(2): 225-246.
Google Scholar: Author Only Title Only Author and Title

Sanz-Martín, J. M., J. R. Pacheco-Arjona, V. Bello-Rico, W. A. Vargas, M. Monod, J. M. Díaz-Mínguez, M. R. Thon and S. A. Sukno (2016). "A highly conserved metalloprotease effector enhances virulence in the maize anthracnose fungus Colletotrichum graminicola." Molecular Plant Pathology 17(7): 1048-1062.
Google Scholar: Author Only Title Only Author and Title

Savojardo, C., P. L. Martelli, P. Fariselli and R. Casadio (2018). "DeepSig: deep learning improves signal peptide detection in proteins." Bioinformatics 34(10): 1690-1696.
Google Scholar: Author Only Title Only Author and Title

Schmidt, S. M., H. Kuhn, C. Micali, C. Liller, M. Kwaaitaal and R. Panstruga (2014). "Interaction of a B lumeria graminis f. sp. hordei effector candidate with a barley ARF-GAP suggests that host vesicle trafficking is a fungal pathogenicity target." Molecular plant pathology 15(6): 535-549.
Google Scholar: Author Only Title Only Author and Title

Sharpee, W., Y. Oh, M. Yi, W. Franck, A. Eyre, L. H. Okagaki, B. Valent and R. A. Dean (2017). "Identification and characterization of suppressors of plant cell death (SPD) effectors from Magnaporthe oryzae." Molecular plant pathology 18(6): 850-863.
Google Scholar: Author Only Title Only Author and Title

Shaw, M. W., S. J. Bearchell, B. D. L. Fitt and B. A. Fraaije (2008). "Long-term relationships between environment and abundance in wheat of Phaeosphaeria nodorum and Mycosphaerella graminicola." New Phytologist 177(1): 229-238.
Google Scholar: Author Only Title Only Author and Title

Shi, G., T. L. Friesen, J. Saini, S. S. Xu, J. B. Rasmussen and J. D. Faris (2015). "The wheat Snn7 gene confers susceptibility on recognition of the Parastagonospora nodorum necrotrophic effector SnTox7." The Plant Genome 8(2): plantgenome2015.2002.0007.
Google Scholar: Author Only Title Only Author and Title

Solomon, P. S., R. G. T. Lowe, K.-C. Tan, O. D. C. Waters and R. P. Oliver (2006). "Stagonospora nodorum: cause of stagonospora nodorum blotch of wheat." Molecular Plant Pathology 7(3): 147-156.
Google Scholar: Author Only Title Only Author and Title

Sommerhalder, R. J., B. A. McDonald and J. Zhan (2006). "The frequencies and spatial distribution of mating types in Stagonospora nodorum are consistent with recurring sexual reproduction." Phytopathology 96(3): 234-239.
Google Scholar: Author Only Title Only Author and Title

Sperschneider, J., A.-M. Catanzariti, K. DeBoer, B. Petre, D. M. Gardiner, K. B. Singh, P. N. Dodds and J. M. Taylor (2017). "LOCALIZER: subcellular localization prediction of both plant and effector proteins in the plant cell." Scientific reports 7(1): 1-14.

Google Scholar: Author Only Title Only Author and Title

Sperschneider, J., P. N. Dodds, D. M. Gardiner, K. B. Singh and J. M. Taylor (2018). "Improved prediction of fungal effector proteins from secretomes with EffectorP 2.0." Molecular plant pathology 19(9): 2094-2110.
Google Scholar: Author Only Title Only Author and Title

Sperschneider, J., P. N. Dodds, K. B. Singh and J. M. Taylor (2018). "ApoplastP: prediction of effectors and plant proteins in the apoplast using machine learning." New Phytologist 217(4): 1764-1778.
Google Scholar: Author Only Title Only Author and Title

Sperschneider, J., D. M. Gardiner, P. N. Dodds, F. Tini, L. Covarelli, K. B. Singh, J. M. Manners and J. M. Taylor (2016). "EffectorP: predicting fungal effector proteins from secretomes using machine learning." New Phytologist 210(2): 743-761.
Google Scholar: Author Only Title Only Author and Title

Sperschneider, J., D. M. Gardiner, L. F. Thatcher, R. Lyons, K. B. Singh, J. M. Manners and J. M. Taylor (2015). "Genome-Wide Analysis in Three Fusarium Pathogens Identifies Rapidly Evolving Chromosomes and Genes Associated with Pathogenicity." Genome Biology and Evolution 7(6): 1613-1627.
Google Scholar: Author Only Title Only Author and Title

Standage, D. S. and V. P. Brendel (2012). "ParsEval: parallel comparison and analysis of gene structure annotations." BMC Bioinformatics 13(1): 187.
Google Scholar: Author Only Title Only Author and Title

Stanke, M., M. Diekhans, R. Baertsch and D. Haussler (2008). "Using native and syntenically mapped cDNA alignments to improve de novo gene finding." Bioinformatics 24(5): 637-644.
Google Scholar: Author Only Title Only Author and Title

Steinbiss, S., U. Willhoeft, G. Gremme and S. Kurtz (2009). "Fine-grained annotation and classification of de novo predicted LTR retrotransposons." Nucleic Acids Research 37(21): 7002-7013.
Google Scholar: Author Only Title Only Author and Title

Steinegger, M. and J. Söding (2017). "MMseqs2 enables sensitive protein sequence searching for the analysis of massive data sets." Nature Biotechnology 35(11): 1026-1028.
Google Scholar: Author Only Title Only Author and Title

Stergiopoulos, I., Y. A. Kourmpetis, J. C. Slot, F. T. Bakker, P. J. De Wit and A. Rokas (2012). "In silico characterization and molecular evolutionary analysis of a novel superfamily of fungal effector proteins." Molecular Biology and Evolution 29(11): 3371-3384.
Google Scholar: Author Only Title Only Author and Title

Stukenbrock, E. H., S. Banke and B. A. McDonald (2006). "Global migration patterns in the fungal wheat pathogen Phaeosphaeria nodorum." Mol Ecol 15(10): 2895-2904.
Google Scholar: Author Only Title Only Author and Title

Syme, R. A., K.-C. Tan, J. K. Hane, K. Dodhia, T. Stoll, M. Hastie, E. Furuki, S. R. Ellwood, A. H. Williams, Y.-F. Tan, A. C. Testa, J. J. Gorman and R. P. Oliver (2016). "Comprehensive Annotation of the Parastagonospora nodorum Reference Genome Using Next-Generation Genomics, Transcriptomics and Proteogenomics." PLOS ONE 11(2): e0147221.
Google Scholar: Author Only Title Only Author and Title

Syme, R. A., K.-C. Tan, K. Rybak, T. L. Friesen, B. A. McDonald, R. P. Oliver and J. K. Hane (2018). "Pan-Parastagonospora Comparative Genome Analysis-Effector Prediction and Genome Evolution." Genome Biology and Evolution 10(9): 2443-2457.
Google Scholar: Author Only Title Only Author and Title

Tan, K.-C., R. P. Oliver, P. S. Solomon and C. S. Moffat (2010). "Proteinaceous necrotrophic effectors in fungal virulence." Functional Plant Biology 37(10): 907-912.
Google Scholar: Author Only Title Only Author and Title

Tan, K.-C., O. D. Waters, K. Rybak, E. Antoni, E. Furuki and R. P. Oliver (2014). "Sensitivity to three Parastagonospora nodorum necrotrophic effectors in current Australian wheat cultivars and the presence of further fungal effectors." Crop and Pasture Science 65(2): 150-158.
Google Scholar: Author Only Title Only Author and Title

Team, R. C. (2013). "R: A language and environment for statistical computing."

Testa, A. C., J. K. Hane, S. R. Ellwood and R. P. Oliver (2015). "CodingQuarry: highly accurate hidden Markov model gene prediction in fungal genomes using RNA-seq transcripts." BMC Genomics 16(1): 170.
Google Scholar: Author Only Title Only Author and Title

Testa, A. C., R. P. Oliver and J. K. Hane (2016). "OcculterCut: a comprehensive survey of AT-rich regions in fungal genomes." Genome biology and evolution 8(6): 2044-2064.
Google Scholar: Author Only Title Only Author and Title

Thioulouse, J., D. Chessel, S. Dole and J.-M. Olivier (1997). "ADE-4: a multivariate analysis and graphical display software." Statistics and computing 7(1): 75-83.
Google Scholar: Author Only Title Only Author and Title

Thrall, P. H., L. G. Barrett, P. N. Dodds and J. J. Burdon (2016). "Epidemiological and Evolutionary Outcomes in Gene-for-Gene and Matching Allele Models." Frontiers in Plant Science 6.

Trainor, G., C. Zaicou-Kunesch, J. Curry, B. Shackley and D. Nicol (2018). 2019 Wheat variety sowing guide for Western Australia, Department of Primary Industries and Regional Development.

Urban, M., A. Cuzick, J. Seager, V. Wood, K. Rutherford, S. Y. Venkatesh, N. De Silva, M. C. Martinez, H. Pedro and A. D. Yates (2020). "PHI-base: the pathogen–host interactions database." Nucleic acids research 48(D1): D613-D620.
Google Scholar: Author Only Title Only Author and Title

Virtanen, P., R. Gommers, T. E. Oliphant, M. Haberland, T. Reddy, D. Cournapeau, E. Burovski, P. Peterson, W. Weckesser, J. Bright, S. J. van der Walt, M. Brett, J. Wilson, K. Jarrod Millman, N. Mayorov, A. R. J. Nelson, E. Jones, R. Kern, E. Larson, C. J. Carey, İ. Polat, Y. Feng, E. W. Moore, J. Vand erPlas, D. Laxalde, J. Perktold, R. Cimrman, I. Henriksen, E. A. Quintero, C. R. Harris, A. M. Archibald, A. H. Ribeiro, F. Pedregosa, P. van Mulbregt and S. Contributors (2020). "SciPy 1.0: Fundamental Algorithms for Scientific Computing in Python." Nature Methods 17: 261-272.
Google Scholar: Author Only Title Only Author and Title

Vleeshouwers, V. G. A. A. and R. P. Oliver (2014). "Effectors as Tools in Disease Resistance Breeding Against Biotrophic, Hemibiotrophic, and Necrotrophic Plant Pathogens." Molecular Plant-Microbe Interactions 27(3): 196-206.
Google Scholar: Author Only Title Only Author and Title

Voigt, C. A., W. Schäfer and S. Salomon (2005). "A secreted lipase of Fusarium graminearum is a virulence factor required for infection of cereals." The Plant Journal 42(3): 364-375.
Google Scholar: Author Only Title Only Author and Title

Wang, Y., J. Wu, S. G. Kim, K. Tsuda, R. Gupta, S.-Y. Park, S. T. Kim and K. Y. Kang (2016). "Magnaporthe oryzae-Secreted Protein MSP1 Induces Cell Death and Elicits Defense Responses in Rice." Molecular Plant-Microbe Interactions 29(4): 299-312.
Google Scholar: Author Only Title Only Author and Title

Waterhouse, R. M., M. Seppey, F. A. Simão, M. Manni, P. Ioannidis, G. Klioutchnikov, E. V. Kriventseva and E. M. Zdobnov (2018). "BUSCO Applications from Quality Assessments to Gene Prediction and Phylogenomics." Molecular Biology and Evolution 35(3): 543-548.
Google Scholar: Author Only Title Only Author and Title

Wickham, H. (2016). ggplot2: Elegant Graphics for Data Analysis, Springer-Verlag New York.
Google Scholar: Author Only Title Only Author and Title

Wood, D. E., J. Lu and B. Langmead (2019). "Improved metagenomic analysis with Kraken 2." Genome Biology 20(1): 257.
Google Scholar: Author Only Title Only Author and Title

Wood, D. E. and S. L. Salzberg (2014). "Kraken: ultrafast metagenomic sequence classification using exact alignments." Genome Biology 15(3): R46.
Google Scholar: Author Only Title Only Author and Title

Wright, E. S. (2015). "DECIPHER: harnessing local sequence context to improve protein multiple sequence alignment." BMC Bioinformatics 16(1): 322.
Google Scholar: Author Only Title Only Author and Title

Wu, T. D. and C. K. Watanabe (2005). "GMAP: a genomic mapping and alignment program for mRNA and EST sequences." Bioinformatics 21(9): 1859-1875.
Google Scholar: Author Only Title Only Author and Title

Xin, Z. and J. Chen (2012). "A high throughput DNA extraction method with high yield and quality." Plant Methods 8(1): 26.
Google Scholar: Author Only Title Only Author and Title

Xu, G., X. Zhong, Y. Shi, Z. Liu, N. Jiang, J. Liu, B. Ding, Z. Li, H. Kang and Y. Ning (2020). "A fungal effector targets a heat shock–dynamin protein complex to modulate mitochondrial dynamics and reduce plant immunity." Science advances 6(48): eabb7719.
Google Scholar: Author Only Title Only Author and Title

Xu, Y., Y. Zhang, J. Zhu, Y. Sun, B. Guo, F. Liu, J. Huang, H. Wang, S. Dong and Y. Wang (2021). "Phytophthora sojae apoplastic effector AEP1 mediates sugar uptake by mutarotation of extracellular aldose and is recognized as a MAMP." Plant Physiology.

Yin, Y., X. Mao, J. Yang, X. Chen, F. Mao and Y. Xu (2012). "dbCAN: a web resource for automated carbohydrate-active enzyme annotation." Nucleic acids research 40(W1): W445-W451.

Yoshino, K., H. Irieda, F. Sugimoto, H. Yoshioka, T. Okuno and Y. Takano (2012). "Cell Death of Nicotiana benthamiana Is Induced by Secreted Protein NIS1 of Colletotrichum orbiculare and Is Suppressed by a Homologue of CgDN3." Molecular Plant-Microbe Interactions® 25(5): 625-636.
Google Scholar: Author Only Title Only Author and Title

Yu, G., D. K. Smith, H. Zhu, Y. Guan and T. T. Y. Lam (2017). "ggtree: an R package for visualization and annotation of phylogenetic trees with their covariates and other associated data." Methods in Ecology and Evolution 8(1): 28-36.
Google Scholar: Author Only Title Only Author and Title

Zhang, Y., K. Xu, D. Yu, Z. Liu, C. Peng, X. Li, J. Zhang, Y. Dong, Y. Zhang, P. Tian, T. Guo and C. Li (2019). "The Highly Conserved Barley Powdery Mildew Effector BEC1019 Confers Susceptibility to Biotrophic and Necrotrophic Pathogens in Wheat." International Journal of Molecular Sciences 20(18): 4376.

Google Scholar: Author Only Title Only Author and Title

Zhang, Z., T. L. Friesen, S. S. Xu, G. Shi, Z. Liu, J. B. Rasmussen and J. D. Faris (2011). "Two putatively homoeologous wheat genes mediate recognition of SnTox3 to confer effector-triggered susceptibility to Stagonospora nodorum." The Plant Journal 65(1): 27-38.

Google Scholar: Author Only Title Only Author and Title